



UNIVERSIDAD DE INVESTIGACIÓN DE TECNOLOGÍA EXPERIMENTAL YACHAY

Escuela de Ciencias Biológicas e Ingeniería

TÍTULO: Synthesis of chitosan fibers by electrospinning

Trabajo de integración curricular presentado como requisito para la
obtención del título de Ingeniero Biomédico

Autor

Dulexy Dayana Solano Orrala

Tutor:

Dr. rer. nat. Julio C. Chacón-Torres

Co-tutor:

MSc. Luis Gerardo Corredor González

MSc. Ana Carmen Valbuena Inciarte

Urcuquí, Agosto, 2023

AUTORÍA

Yo, **SOLANO ORRALA DULEXY DAYANA**, con cédula de identidad 2450580309, declaro que las ideas, juicios, valoraciones, interpretaciones, consultas bibliográficas, definiciones y conceptualizaciones expuestas en el presente trabajo; así cómo, los procedimientos y herramientas utilizadas en la investigación, son de absoluta responsabilidad de el/la autora (a) del trabajo de integración curricular. Así mismo, me acojo a los reglamentos internos de la Universidad de Investigación de Tecnología Experimental Yachay.

Urcuquí, Agosto, 2023.

Dulexy Dayana Solano Orrala

CI: 2450580309

AUTORIZACIÓN DE PUBLICACIÓN

Yo, **SOLANO ORRALA DULEXY DAYANA**, con cédula de identidad 2450580309, cedo a la Universidad de Investigación de Tecnología Experimental Yachay, los derechos de publicación de la presente obra, sin que deba haber un reconocimiento económico por este concepto. Declaro además que el texto del presente trabajo de titulación no podrá ser cedido a ninguna empresa editorial para su publicación u otros fines, sin contar previamente con la autorización escrita de la Universidad.

Asimismo, autorizo a la Universidad que realice la digitalización y publicación de este trabajo de integración curricular en el repositorio virtual, de conformidad a lo dispuesto en el Art. 144 de la Ley Orgánica de Educación Superior.

Urcuquí, Agosto, 2023.

Dulexy Dayana Solano Orrala

CI: 2450580309

Dedicatoria

*Para mis padres Darwin S. y Fatima O.
A la memoria de Holger G., Oscar S. y Piero R*

Dulexy Dayana Solano Orrala

Agradecimiento

Son muchas las personas que me ayudaron a culminar mi grado que es poco lo que puedo expresar en este escrito cuando el corazón es el que habla.

A Julio Chacón. PhD por ser mi guía en el desarrollo de este trabajo experimental y brindarme todas las herramientas para culminarlo. Gracias por confiar en mí y motivarme cuando los resultados no eran los que esperábamos. A MSc. Luis Corredor, MSc. Ana Carmen Valbuena, MSc. Marco León, Raúl Dávalos PhD, Carlos Loyo PhD, Empresa Ecuachitosan y al Colegio de Ciencias e Ingenierías de la USFQ por su incontable apoyo en esta investigación. A mis maestros de Yachay por ayudarme a formar una vocación con enfoque al servicio.

A mis padres, por no escatimar esfuerzos para apoyarme en absolutamente todo. Gracias por brindarme una familia llena de oportunidades para crecer profesionalmente y en virtud. A mis amigos de la escuela verde, no conozco biomédicos más talentosos que ustedes. A Gabriela Rocha y María Belen Terán, gracias por ayudarme a crecer en espíritu. A Pablo Urbano, por ser soporte y ayudarme en los momentos claves. A Geomara Rodríguez por su nobleza y bonita amistad. Y a todas las personas que me acompañaron y vivieron conmigo estos últimos 5 años, fueron luz verdaderamente.

Esta etapa ha puesto mi alma en dirección y me ha llenado de bonitas experiencias. Gracias a Dios por dejarme vivir su vida, ser tan bueno conmigo y permitirme cumplir los deseos de mi corazón.

Con mucho cariño

Dulexy Dayana Solano Orrala

Resumen

Las fibras de quitosano electrohiladas se han estudiado por su biocompatibilidad y sus propiedades antibacterianas. Sin embargo, la producción de fibras puras de quitosano mediante electrospinning es un reto debido a su rígida estructura química. En este estudio se sintetizan fibras de quitosano optimizando la solución de polímero y los parámetros del proceso de electrospinning. Se elaboraron soluciones a varias concentraciones de quitosano a partir de caparzones de camarón, cangrejo y quitosano comercial (Sigma-Aldrich). Los disolventes usados fueron ácido acético diluido (AcOH), ácido trifluoroacético (TFA) al 99 % de pureza y diclorometano (DCM). Para mejorar su conductividad, algunas soluciones se reforzaron con nanotubos de carbono multipared (MWCNT). Se probaron varias soluciones de quitosano para electrospinning, pero ninguna produjo un chorro visible cuando se aplicó el campo eléctrico. Sólo cuando se utilizó TFA como disolvente se depositaron fibras de quitosano en el colector. La homogeneidad de las fibras electrohiladas se mejoró añadiendo DCM a la solución de quitosano-TFA. Mediante microscopía electrónica de barrido (SEM) se analizó la morfología de las fibras; antes de la observación, las muestras se recubrieron de oro mediante pulverización de plasma. Las muestras que proporcionaron las mejores fibras fueron de quitosano de Sigma-Aldrich y quitosano de cangrejo a una concentración del 4% (p/v) utilizando TFA/DCM como solvente. Al someter las fibras a un análisis químico mediante espectroscopia Raman, los resultados indicaron la presencia de grupos amino (NH_2) característicos del quitosano. Es interesante observar que los picos relacionados con el solvente (CF_3) no eran visiblemente prominentes en los espectros, lo que indica que el proceso de electrospinning consiguió eliminar el solvente. La producción satisfactoria de fibras de quitosano ofrece un nuevo enfoque para crear andamios inteligentes para la ingeniería de tejidos.

Palabras claves: Quitosano, electrohilado, biomaterial, solvente,

Abstract

Electrospun fibers based on chitosan have been studied for their biocompatibility and antibacterial properties. Nevertheless, producing pure chitosan fibers through electrospinning is challenging due to its rigid chemical structure. This study synthesizes chitosan fibers by optimizing polymer solution and electrospinning process parameters. Several concentrations of chitosan were produced from shrimp, crab shells, and commercial chitosan(Sigma-Aldrich). The solvents tested were dilute Acetic Acid (AcOH), Trifluoroacetic acid (TFA) 99 % purity, and Dichloromethane (DCM) . To improve their conductivity, some solutions were reinforced with Multi Walled Carbon Nanotubes (MWCNTs). Several chitosan solutions were tested for electrospinning, but none produced a visible jet when the electric field was applied. Only when TFA was used as the solvent, chitosan fibers were deposited onto the collector. The results showed that when the chitosan concentration was increased, the morphology of the deposition on the collector changed from spherical beads to interconnected fiber. The homogeneity of the electrospun chitosan fiber was improved by adding DCM to the chitosan-TFA solution with a volume ratio 70:30 v/v. Scanning electron microscopy (SEM) analyzed the morphology of the fibers; before observation, the samples were coated with gold using plasma sputtering. The samples that provided the best fibers were Sigma-Aldrich chitosan and crab chitosan at a concentration of 4 % (w/v) using TFA/DCM as solvent. Upon subjecting the fibers to chemical analysis via Raman spectroscopy, the results indicated the presence of amino groups (NH₂) that are characteristic of chitosan. It is interesting to note that the solvent-related peaks (CF₃) were not visibly prominent in the spectra, indicating that the electrospinning process was successful in eliminating all the solvent. The successful production of chitosan fibers offers a new approach to creating smart scaffolds for tissue engineering.

Keywords: Chitosan, electrospinning, biomaterial, solvent,

Contents

List of Figures	xv
List of Tables	xviii
1 Introduction	1
1.1 Problem Statement	2
1.2 Motivation and Research Objectives	4
1.2.1 General Objective	4
1.2.2 Specific Objectives	4
2 Theoretical Background	5
2.1 Chitosan	5
2.2 Source	5
2.3 Production of Chitosan	6
2.4 Properties of chitosan biopolymers	7
2.5 Structure–properties relationship	8
2.6 Remarkable properties of chitosan as biomaterial	8
2.7 Electrospinning	11
2.7.1 Electrospinning Process	11
2.7.2 Electrospinning Principles	13

2.8	Parameters of electrospinning process	15
2.8.1	Viscosity/concentration	15
2.8.2	Polymer molecular weight	16
2.8.3	Flow rate	16
2.8.4	Field strength/voltage	16
2.8.5	Distance between tip and collector	17
2.8.6	Collector composition and geometry	17
2.8.7	Ambient parameters	17
2.9	Electrospinning of chitosan for Biomedical application	18
2.9.1	Composite scaffolds	18
2.9.2	Co-polymer scaffolds	18
2.9.3	Commercial chitosan products	19
3	Methodology	21
3.1	Materials	21
3.2	Electrospinning solution	23
3.2.1	Chitosan in AcOH	26
3.2.2	Chitosan +MWCNT in AcOH	26
3.2.3	Chitosan in TFA and TFA/DCM	26
3.3	Electrospinning	27
3.4	Characterization	27
3.4.1	Scanning Electron Microscopy (SEM)	29
3.4.2	Raman spectroscopy	30
4	Results & Discussion	35
4.1	Optimising the polymer solutions and process parameters	35
4.2	Scanning Electron Microscopy	45

4.3 Raman Spectroscopy	50
5 Conclusions & Outlook	57
5.1 Recomendations and future work	59
A Electrospinning processing data	61
B WET SPINNING	73
Bibliography	77

List of Figures

2.1	Schematic representation of chitosan.	6
2.2	Chitosan production process	7
2.3	Chitosan in biomedical field	10
2.4	Electrospinning apparatus	12
3.1	Experimentation flowchart	22
3.2	Illustration of the fiber synthesis process carries out by electrospinning.	23
3.3	Electrospinning unit at Yachay Tech University	29
3.4	Fiber sample preparation for SEM	30
3.5	Scanning Electron Microscopy (SEM) illustration	31
3.6	108C Auto/SE Carbon Coater equipment	32
3.7	LabRAM HR Evolution Raman microscope	33
4.1	Mixture of chitosan with solvent.	36
4.2	Chemical reaction of chitosan dissolved in AcOH	37
4.3	Time for chitosan to dissolve in AcOH	38
4.4	MWCNT-reinforced chitosan samples	38
4.5	SEM photograph of the deposited chitosan using AcOH as solvent.	39
4.6	The chemical reaction between chitosan and TFA	40
4.7	Time for chitosan to dissolve in TFA and TFA/DCM	41

4.8	Evaluation of the surface tension of the polymeric solution	43
4.9	Shape of the polymer solution jet at different processing parameters. Chitosan/TFA solution	44
4.10	Relationship between the concentration of chitosan and the dissolution time	45
4.11	Electrospun Sigma-Aldrich Chitosan 4% (w/v) TFA: DCM	46
4.12	Electrospun Crab Chitosan 4% (w/v) TFA: DCM	47
4.13	Fiber diameter histogram	48
4.14	Raman spectra of Sigma Aldrich chitosan fibers made by electrospinning using TFA as solvent	51
4.15	Raman spectra of Sigma Aldrich chitosan fibers made by electrospinning using TFA:DCM as solvent	53
4.16	Raman spectra of crab chitosan fibers made by electrospinning TFA:DCM	55
B.1	Raman Spectra of Sigma Aldrich chitosan fibers made by wet spinning	74

List of Tables

3.1	Chitosan samples using AcOH as solvent	24
3.2	Chitosan samples using TFA and DCM as solvent.	25
3.3	Step-by-step procedure for operating electrospinning.	28
4.1	Dielectric constant and boiling point of the solvents	40
4.2	Processing parameters of chitosan samples with better electrospun fiber performance. . .	42
4.3	Raman peaks assigned to the bands	54
A.1	ACOH Commercial chitosan samples	62
A.2	ACOH Shrimp Chitosan Samples	63
A.3	ACOH Crab chitosan Samples	64
A.4	ACOH Commercial chitosan+MWCNT samples	65
A.5	ACOH Shrimp chitosan+MWCNT samples	66
A.6	ACOH Crab chitosan+MWCNT samples	67
A.7	TFA Commercial chitosan samples	68
A.8	TFA Crab chitosan samples	69
A.9	TFA/DCM Commercial chitosan samples	70
A.10	TFA/DCM Crab chitosan samples	71
B.1	Chitosan fiber made by the wet spinning technique using AcOh as solvent	75

Chapter 1

Introduction

In recent years, there has been significant scientific interest worldwide in biomaterials like chitosan, starch, collagen, gelatin, alginate, and cellulose. These materials are attractive candidates for use in biomedical fields due to their ability to support cell adhesion, migration, proliferation, and differentiation effectively¹. Chitosan is an extensively used natural polysaccharide that has garnered noteworthy recognition for its advantageous features, including biocompatibility, biodegradability, and its effectiveness in combating bacteria and inflammation². The antimicrobial properties of chitosan oligomers are enhanced due to the polymer chain's positive charges and free amino groups. Therefore, increasing the number of amino groups improves antimicrobial activity by changing the bacterial cell wall's permeability. Protonated amine groups of chitosan bind negatively charged bacteria breaking their reproduction³.

The conventional fiber spinning methods are melt spinning, wet spinning, and dry spinning⁴. Recently, there has been a lot of focus on using high electrostatic potentials to create ultrafine fibers from various materials through a process called electrospinning. Chitosan-based electrospun nanofibers have been extensively studied, and many products containing chitosan nanofibers have been made through electrospinning.

Producing high-quality chitosan nanofibers is difficult due to their inflexible chemical structure, positively charged properties, and intricate hydrogen bonding at the molecular level⁵. In electrospinning, the solvent plays two essential roles. Firstly, it dissolves the polymer molecules, making them ready to form an electrified jet. Secondly, it transports the dissolved polymer molecules towards the collector and then rapidly vaporizes to leave behind the polymer fibers. Choosing the right solvent system is crucial for successful electrospinning⁶.

The research aims to create pure chitosan fibers using 3 types of chitosan sources: 1) shrimp chitosan, 2) crab chitosan, and 3) commercial chitosan.

1.1 Problem Statement

Chitosan is one of the most abundant natural polysaccharides, and the global market volume is expected to reach USD 47.06 billion by 2030⁷. Chitosan is a highly sought-after material due to its unique properties, which make it biologically renewable, biodegradable, and non-toxic. It is also biocompatible, non-antigenic, and biofunctional. These properties are essential in successfully electrospinning the material and help bridge the gap between basic polymer chemistry and advanced nanomaterial science⁸.

Although many articles have been published during the last twenty years, fiber chitosan applications in the biomedical field still need to be improved, mainly due to the difficulty of obtaining fiber with high purity⁹. The high electric field involved in electrospinning causes repulsion among the ionic groups present in the polymer backbone. As a result, bead formation occurs frequently, which makes it quite challenging to create pure chitosan nanofibers in a continuous form¹. Moreover, the production of uniform fibers using chitosan-based materials poses a significant challenge due to the complexity of selecting appropriate solvents and ensuring robustness based on fiber properties, processing parameters, and solution concentration. Consequently, the production of chitosan-based materials is relatively limited due to their higher cost compared to synthetic polymers¹. For this reason, developing more economical and environmentally friendly methods to obtain chitosan and convert it into valuable products is required.

Research on chitosan is crucial in Ecuador due to its abundant raw material resources, especially white shrimp. With an annual production of 600-800 million pounds, chitosan is the country's second-largest non-oil export¹⁰. The majority of shrimp is sold with its exoskeleton still intact, accounting for 62% of sales. 87% of the national shrimp production is exported, while the remaining 13% is sold locally. In Ecuador, the shrimp exoskeleton is considered a waste in most food industries. The exoskeleton represents approximately 15-20% of the total weight of the shrimp; however, waste from shrimp processing is about 40-50% of its weight (this includes the exoskeleton, legs, head, and tail); this means that a minimum of 41,000 tons of shrimp waste are wasted annually, which could be used in the production of chitosan¹¹.

According to Mathur Narang¹² it requires 10 kilograms of shrimp waste to manufacture 1 kilogram of chitosan via chemical deacetylation. This implies that Ecuador has the potential to generate 4,100 tons of chitosan annually. To provide insight into the economic opportunity, a quantity of 250 grams of chitosan can be sold for USD 231, which could result in a net profit of roughly USD 1.5 billion after factoring in the expenses related to production and raw materials.

It is important to conduct research in Ecuador regarding the industrial extraction and production of chitosan. This research can help create finished products like filters and dressings that use the electrospinning technique to generate nanofibrous membranes¹³. The electrospinning process has gained more attention from the scientific community in the last three decades due to its unique advantages that generate promising results, especially in nanotechnology and biomedicine. Research on electrospinning is mainly led by the United States, as evidenced by the increasing number of scientific publications.

However, in Ecuador, there needs to be more research on electrospinning. The educational institutions that lead the field are the Yachay Tech University and the Universidad de las Fuerzas Armadas - ESPE. This demonstrates the feasibility, viability, and importance of the current project since it would lay the foundations for future research aimed at applying the results of this study in biomaterials, tissue engineering,

drug delivery, and wound healing. Additionally, there is a growing demand to study and industrialize the manufacturing methods of biomaterials derived from shrimp to gain better knowledge of the raw material and eventually market the products.

1.2 Motivation and Research Objectives

1.2.1 General Objective

Synthesize pure chitosan fibers by electrospinning technique for biomedical application.

1.2.2 Specific Objectives

- To determine the most optimal parameters of the chitosan solution (molecular weight, solvent, and viscosity/concentration) and processing (voltage, flow rate, and distance between needle tip and collector) to make pure chitosan fibers by electrospinning.
- To improve the electrospinning properties of the solution by adding Multi Walled Carbon Nanotubes (MWCNTs)
- To evaluate the morphological characteristics of the fibers obtained using Scanning electron microscopy (SEM)
- To analyze the chemical composition and functional groups present in chitosan fibers by Raman spectroscopy to understand the role of the electrospinning process and the interaction between chitosan and the solvent in the resulting fibers.

Chapter 2

Theoretical Background

2.1 Chitosan

Chitosan is a natural biopolymer derived from the chitin deacetylation, found on crustacean shells (e.g., shrimps, lobsters and crabs)⁷. It consists of D-glucosamine and N-acetyl D-glucosamine linked through a β -1,4-glycosidic bond, as depicted in Figure 2.1. The presence of reactive amino groups at C2 atom and the hydroxyl group at atom C3 and C6 on chitosan is useful in a wide application in various industries. This natural polysaccharide has attracted much attention in numerous biomedical applications because of its well-known exceptional biocompatibility, non-toxicity, antimicrobial activity against a wide range of bacteria and fungi, nonimmunogenicity and readily biodegradability⁶. Degree of Deacetylation (DD) in chitosan can range from 40% DD to 98% DD, while its Molecular Weight (MW) can range from 50 Kilodalton (kDa) to 2000 kDa.

2.2 Source

Chitosan can be extracted from multiple sources, including insects, yeast, mushrooms, cell walls of fungi, and marine shellfish such as crabs, lobsters, krill, cuttlefish, shrimps, and squid pens. Chitin forms a

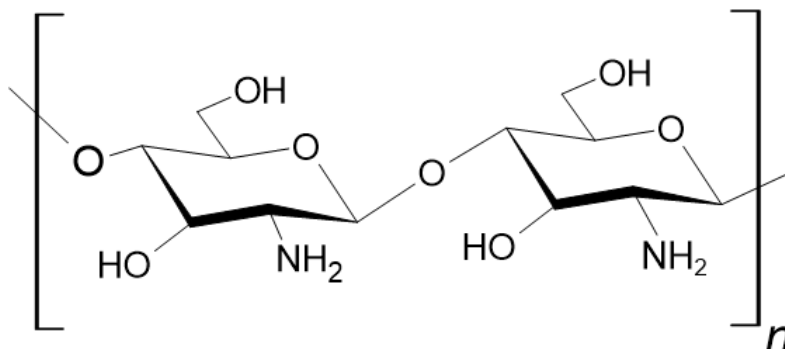


Figure 2.1: Schematic representation of chitosan.

covalently bound network with proteins, metals, and carotenoids in shellfish to create an outer protective coating. The shells of crustaceans contain 30-40 % proteins, 30-50% calcium carbonate, and 20-30 % chitin. They also have different pigments like astaxanthin, canthaxanthin, lutein, and carotene, but their proportions vary depending on the species and seasons. Shrimp, prawn, and crab waste are the primary sources of commercial chitin and chitosan production due to the increase in shellfish consumption and the expansion of aquaculture. Nonetheless, mycelium waste from fermentation processes presents an untapped potential source.

2.3 Production of Chitosan

Chitosan production involves several steps, including the preparation of chitin from biological material, followed by deacetylation to produce chitosan. Typically, the production process for chitosan from crustacean shells involves four basic steps: demineralization, deproteinization, decoloration, and deacetylation. The order of demineralization and deproteinization steps can be interchangeable. The exoskeleton of crustaceans is a commonly used starting material for commercial chitosan production. Figure 2.2 clearly depicts the process of chitosan powder production, which begins with the extraction of chitosan from crustacean shell.

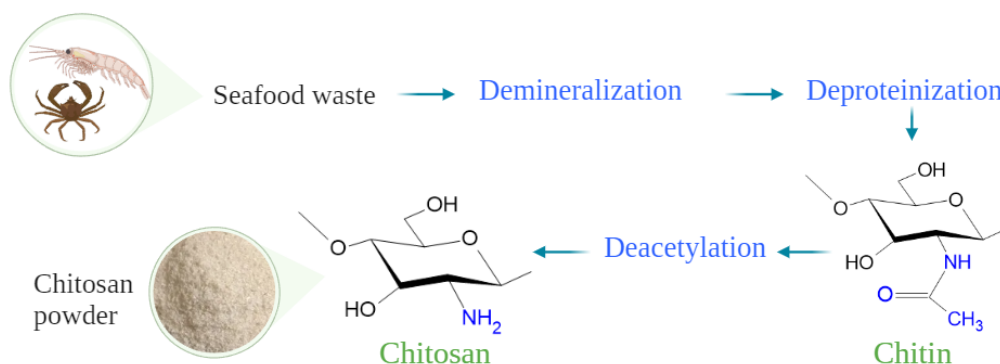


Figure 2.2: Chitosan production process

2.4 Properties of chitosan biopolymers

Chitosan is powder (or flakes) with different MW, DD, insoluble in water and organic solvents, soluble in dilute hydrochloric, formic and Acetic Acid (AcOH). The solubility of chitosan depends on MW and DD¹⁴. Understanding the molecular weight of polysaccharides is crucial for comprehending their applications and functions in living systems. The molecular weight of chitosan is heavily influenced by the conditions of deacetylation. Chitosan is available commercially with molecular weight ranging from 10 to 1000 kDa. The higher the DD of chitosan, the higher the degree of protonation of amino groups in the molecule, and the easier it dissolves. The larger chitosan MW, the more hydrogen bonds form in its polymer chain, and the more difficult it dissolves. The viscosity of chitosan rises when its molecular weight and concentration increase. Additionally, the degree of deacetylation also has a positive effect on viscosity.

Chitosan stands out among other polysaccharides due to its numerous beneficial properties. These include non-toxicity, chelating activities, biocompatibility, biodegradability, adsorption capacities, film-

forming ability, and bacteriostatic action¹⁵. Chitosan has been shown to possess antiviral and antibacterial properties. Additionally, its derivatives have been found to have immunostimulating, adjuvant, adaptogenic, anti hypoxic, cholestric, radioprotective, and hemostatic effects.

2.5 Structure–properties relationship

The antimicrobial properties of chitosan are due to the presence of amino groups in its structure. In an acid environment, the NH_2 groups in the C2 position of chitosan protonates to yield NH_3^+ , which binds to negatively charged carboxylate ($-COO^-$) groups located on the surface of the bacterial and fungal cell surfaces, causing disruption of the barrier properties of the outer membranes of the microorganisms followed by leakage of cell components¹⁶. This hypothesis is supported by electron microscopy studies that show binding of chitosan to outer membrane of bacteria¹⁷.

2.6 Remarkable properties of chitosan as biomaterial

As already mentioned, several remarkable properties of chitosan offer unique opportunities for developing biomedical applications. The elucidation of their mechanism will lead to a better understanding of chitosan medical and pharmaceutical interests¹⁸. Due to its positive charges, chitosan can also interact with the negative part of the cell membrane, which can lead to reorganization and an opening of the tight junction proteins, explaining the permeation-enhancing property of this polysaccharide. As for mucoadhesion, if chitosan DD increases, the permeation ability also increases¹⁹. The case of chitosan antimicrobial activity is slightly more complex; two main mechanisms have been reported in the literature to explain chitosan antibacterial and antifungal activities.

In the first proposed mechanism, positively charged chitosan can interact with negatively charged groups at the surface of cells and, as a consequence, alter its permeability²⁰. This would prevent essential materials from entering the cells or/and lead to leaking total solutes out of the cell. The second mechanism

involves chitosan binding with the cell DNA (still via protonated amino groups), which would lead to the inhibition of microbial RNA synthesis. Chitosan antimicrobial properties might result from combining both mechanisms.

The polycationic nature of chitosan also allows explaining chitosan analgesic effects. Indeed, the amino groups of the D-glucosamine residues can protonate in the presence of proton ions released in the inflammatory area, resulting in an analgesic effect²¹. To explain chitosan biodegradability, it is important to remember that chitosan is not only a polymer bearing amino groups but also a polysaccharide, which consequently contains breakable glycosidic bonds. Chitosan is degraded *in vivo* by several proteases, mainly lysozyme²².

The biodegradation of chitosan leads to the formation of non-toxic oligosaccharides of variable length²³. To explain the relationship between chitosan biodegradation and DD, it is important to remember that chitosan is a semi-crystalline polymer; crystallinity is indeed maximum for a DD equal to 0 or 100% (chitin or fully deacetylated chitosan, respectively), and decreases for intermediate DD. Yet, as polymer crystallinity is inversely related to the biodegradation kinetic, when chitosan DD decreases (close to 60%), its crystallinity also decreases, which increases the biodegradation rate. Besides, the distribution of acetyl residues along chitosan will also affect its crystallinity and, consequently, the biodegradation rate²⁴.

Due to its properties, Chitosan has been widely tested in biomedical and pharmaceutical applications, including sutures, dental and bone implants, and artificial skin. Some applications of chitosan in the biomedical field are shown in Figure 2.3. The U.S. Food and Drug Administration (FDA) has approved it for use in wound dressings because of its biocompatibility²⁵. However, its compatibility with the body depends on how it is prepared, as residual proteins can cause allergic reactions, and the biocompatibility increases with an increase in DD. *In vitro* studies have shown that Chitosan is more cytocompatible than chitin⁸, and the interaction between cells and chitosan improves with an increase in positive charges²⁶.

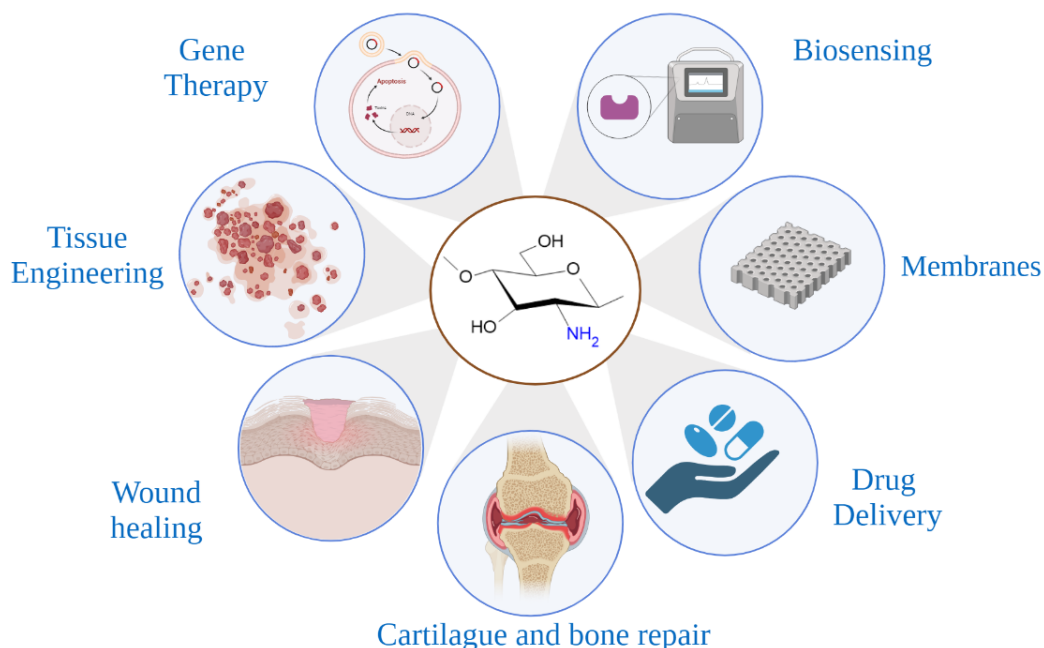


Figure 2.3: Chitosan in biomedical field

When creating implantable scaffolds, it's important to consider factors such as body compatibility, mechanical properties, scaffold shape and porosity, and its ability to promote healing and tissue replacement²⁷. To meet the requirements for tissue engineering scaffolds, the scaffold must not cause any adverse reactions, be biodegradable, have surface properties that encourage cell growth, possess suitable mechanical properties, and be available in various shapes. Chitosan is a promising biomaterial for creating scaffolds because it can replace damaged tissue and promote cell attachment and growth. However, it's essential to use robust processing methods to adjust the scaffold properties to meet the needs of the diseased tissue. In this article, we'll review the different techniques for shaping chitosan hydrogels and foams to create 3D-scaffolds suitable for tissue engineering.

2.7 Electrospinning

Electrospinning has been used for more than 60 years to generate polymer fibers by utilizing electrostatic forces²⁸. Its applications in protective filtration, electronics, catalysis, clothing, biomedicine, and agriculture continue to pique people's interest. The following are the main benefits of this top-down nanotechnology: (1) constant nanofibers in comparison with other bottom-up techniques ; (2) uniform nanofibers that do not require expensive purification; and (3) low cost. Under high electric fields, the electrospinning technique could produce constant polymeric nanofibers from melts of polymer or solutions. An electrospinning setup usually includes a spinneret, a high-voltage power supply, a grounded target, and syringe pumps. Many variables influence the electrospinning process.

2.7.1 Electrospinning Process

The apparatus used for electrospinning consists of a high-voltage power supply with positive or negative polarity, a needle spinneret connected to the syringe with a polymer reservoir, and a conducting flat plate or rotating drum that acts as a ground collector (see Fig2.4). The polymer solution or melt is held by its surface tension in the form of a droplet at the needle tip (spinneret). When an electric potential is applied between the needle of the syringe and collector, then increasing the voltage²⁹, the charge is induced on the fluid surface, and the pendant droplet of the polymer solution at the needle tip is deformed into a conical shape (Taylor cone). This occurs at the equilibrium of the polymer solution or melt's electric forces and surface tension. When the intensity of the electrical fields surpasses a critical value, the electrostatic force will increase the electrical repulsion between the mutual charges on the drop's surface. Thereby, the electrostatic forces will overcome the surface tension of the polymer solution, and consequently, a fine-charged jet is ejected from the cone's apex. Meanwhile, the solvent immediately evaporates, and finally, the jet solidifies into fibers deposited on the collector plate.

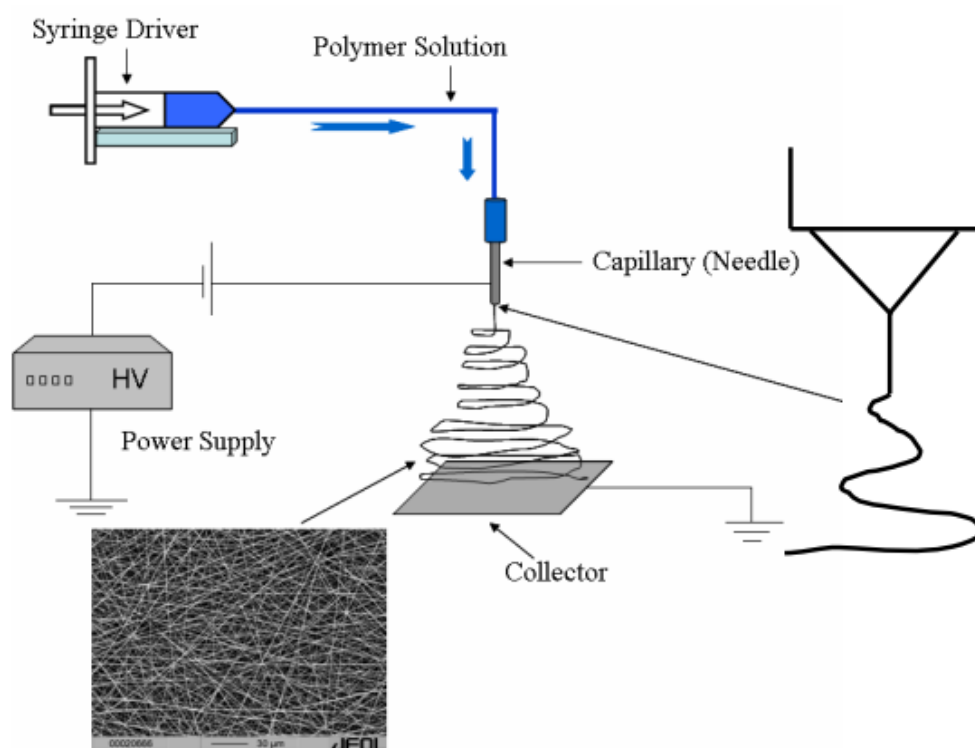


Figure 2.4: Electrospinning apparatus

2.7.2 Electrospinning Principles

The electrospinning process involves three steps: First, a pendant droplet is charged to form a cone-shaped jet in an electric field. Second, the charged jet is elongated under the electric field, which causes the growth of bending instability (also known as whipping instability). Finally, the jet is solidified and collected as solid fibers on a grounded collector³⁰.

The polymer solution is ejected from the spinneret during electrospinning to form a pendant droplet due to surface tension. The droplet is then electrified in the presence of the external electric field, which results in the deformation of the electrified droplet into a conical shape due to the electrostatic repulsion among the surface charges that feature the same sign. Thus, a charged jet is ejected from the tip of the conical shape. Geoffrey Taylor mathematically explained the deformation of a droplet into a conical shape in an external electric field through Plateau-Rayleigh instability between 1964 and 1969³¹. This conical shape is now known as the “Taylor cone.” Equation 2.1 describes the electrostatic pressure (P_e) exerted by the external electric field on the surface of a droplet, assuming the liquid inside the droplet is a perfect conductor.

$$P_e = \varepsilon E^2 / 2 \quad (2.1)$$

where ε represents the dielectric constant of the surrounding medium and E represents the electric field intensity. To calculate the capillary pressure (P_c) caused by surface tension, use the Young-Laplace equation in the form 2.2 ,

$$P_c = 2\gamma / r \quad (2.2)$$

Where γ is the surface tension, and r is the mean radius of curvature of the surface, which approximately equals the inner radius of the spinneret. Once the electric field reaches a specific level known as the critical voltage V_C , the electrostatic repulsion becomes stronger than the surface tension, and the droplet changes

shape into a cone. This can be calculated using the equation 2.3.

$$V_c^2 = \frac{4H^2}{\iota^2} \left(\ln \left(\frac{2\iota}{R} \right) - 1.5 \right) (1.3\pi R\gamma)(0.09) \quad (2.3)$$

where H is the distance between the tip of the spinneret and the collector, ι is the length of the spinneret, and R is the outer radius of the spinneret. Factor 1.3 is obtained using the equation $2\cos 49.3^\circ$, assuming that the cone has a semi-vertical angle of approximately 49.3° , which is believed to be close to its equilibrium value. The properties of the liquid also affect the critical voltage required to deform the droplet into a conical shape³². For a polymer solution to form a Taylor cone during electrospinning, the voltage's electrostatic repulsion threshold must exceed the sum of the liquid's surface tension and viscoelastic force. There must be enough liquid supply to compensate for the ejected amount to maintain the Taylor cone's shape during the process.

When a charged jet is expelled from the Taylor cone, it elongates in a straight line towards the collector due to the electric field and gains acceleration. This linear elongated jet segment is named the near-field region, and the electric force is dominant in this region. The surface tension and viscoelastic force gradually reduce the acceleration in the jet. Meanwhile, because the jet is continuously elongated, its diameter in the straight segment decreases as it moves away from the tip. In this region, The Rayleigh instability should be overcome by the viscoelastic properties of the fluid to prevent the jet from breaking into droplets.

When the acceleration is reduced to zero or a constant, any small perturbation, such as the electrostatic repulsion generated by the surface charges located on the jet, can disturb this straight movement, resulting in the indication's instability of the far-field region. In the far-field area, there are three instabilities: Rayleigh instability (axisymmetric), axisymmetric instability at a higher electric field, and bending instability (whipping, non-axisymmetric)²⁰ Rayleigh instability leads to the potential breakup of the jet into the droplets, governed by surface tension. Rayleigh instability can be suppressed at a strong electric field according to equation 2.3. Bending instability occurs when the aerodynamic instability causes a "lateral electrostatic force" to act perpendicular to the electric field, resulting in wave-like perturbations on the jet.

This force causes the jet to bend, as it is influenced by the electrostatic repulsion between surface charges in a strong electric field, ultimately forming a coil³³.

The last step in electrospinning involves solidifying and collecting the jet as solid fibers. This is achieved by evaporating the solvent, which leads to the solidification of the jet. Fibers with a thinner diameter are produced if the solidification process is slow. The solidified fibers are then collected on a grounded collector, resulting in nonwoven fibrous materials. The morphology of the final product is mainly determined by bending instability. In order to create electrospun nanofibers, it is necessary to induce a bending instability by causing the rapidly growing jet to bend or stretch.

2.8 Parameters of electrospinning process

The properties of electrospun fibers, such as their morphology, diameter, porosity, uniformity, and mechanical properties, depend on various factors. These factors include processing parameters and solution properties. To create desired electrospun fibers, one can systematically vary the electrospinning parameters. The most important factors to consider are the solution properties, which are affected by the polymer's solubility and the solvent's vapor pressure. Additionally, the electrospinnability of the solution is significantly influenced by polymer crystallization, glass transition temperature, molecular weight, and molecular weight distribution. Processing parameters, such as electric field strength, solution feeding rate, needle diameter, and distance between the needle tip and ground collector, also impact the resulting fibers⁹.

2.8.1 Viscosity/concentration

The concentration of polymer in the solution affects the viscosity, which plays a major role in determining the size and shape of polymeric fibers during spinning. When the polymer concentration is low, defects such as beading and droplets can occur, making the process more similar to electrospraying than spinning.

Wet fibers reaching the collector can also indicate the presence of junctions and bundles. Increasing the polymer concentration to increase the solution viscosity is recommended to avoid these issues and achieve uniform fibers with minimal defects¹⁵.

2.8.2 Polymer molecular weight

The molecular weight of the polymer has a significant impact on the properties of the polymer solution and the electrospun product form³⁴, Haghgi and Akbari³⁵, have noted that molecular weight affects the rheological properties (viscosity and surface tension) and the electrical properties (conductivity and dielectric strength). It has been noted that solutions with low molecular weight tend to form beads instead of fibers, while solutions with high molecular weight produce fibers with a larger average diameter.

2.8.3 Flow rate

There have been few comprehensive studies conducted on the correlation between solution feed/flow rate and fiber size and morphology. Generally, it has been observed that lower flow rates lead to smaller diameter fibers, while excessively high flow rates can cause beading due to insufficient drying time before reaching the collector¹².

2.8.4 Field strength/voltage

Among the controlled variables, one of the most studied parameters is the effect of field strength or applied voltage. When the voltage or field strength is low, a drop is usually held at the tip of the needle, and a jet is formed from the Taylor cone, resulting in a smooth spinning process without any beads (provided that the electric field is strong enough to overcome the surface tension).

2.8.5 Distance between tip and collector

An alternative way to control the size and shape of fibers is by adjusting the distance between the tip and the collector. However, it was concluded that fibers need enough time to dry before reaching the collector, which requires a minimum distance. If the distance is too close or too far, beading may occur. According to Korniienko et al. (2022), the size and shape of fibers in gelatin, chitosan, and poly(vinylidene fluoride) are not significantly impacted by the distance between the tip and collector during spinning²⁵.

2.8.6 Collector composition and geometry

When making collectors, using materials like paper and copper mesh will result in less tightly packed structures compared to using aluminum foil or water. Collectors made with a conductive frame have better alignment of fibers than those made with a non-conductive frame³⁶.

2.8.7 Ambient parameters

Few studies have been conducted to examine the effects of ambient parameters (i.e., temperature and humidity) on the electrospinning process. Mit-Uppatham et al. spun polyamide fibers at temperatures ranging from 25 to 60°C. They found that increasing the temperature yielded fibers with a decreased fiber diameter, and they attributed this decline in diameter to the decrease in the viscosity of the polymer solutions at increased temperatures¹. The humidity was varied by Casper et al. while spinning polystyrene solutions. Their work showed that increasing the humidity resulted in the appearance of small circular pores on the surface of the fibers; increasing the humidity further lead to the pores coalescing.

2.9 Electrospinning of chitosan for Biomedical application

Electrospinning chitosan has been challenging due to its rigid D-glucosamine repeat unit, high crystallinity, and ability to hydrogen bond, which result in poor solubility in common organic solvents. To electrospin defect-free fibers from chitosan solutions, the polymer concentration must be at least 2 to 2.5 times the entanglement concentration. However, chitosan solutions at these concentrations are often too viscous to overcome the electric field, making electrospinning difficult. Moreover, chitosan's cationic nature affects the solutions' rheology, and the solution's viscosity must be within a specific window for nanofibers to form successfully. Blending chitosan with other polymers has been proposed to improve the electrospinnability of the solutions by several research groups⁸.

2.9.1 Composite scaffolds

Composite scaffolds can also be created using electrospinning. One type of composite scaffold developed has sought to incorporate carbon nanotubes into the electrospinning process to reinforce polymeric fibers. Composite materials, based on polymer/carbon, are interesting materials because of their enhanced properties, compared to those of the pure polymers. For example, the addition of MWCNTs can enhance a wide range of properties, including the electrical conductivity of a selected polymeric matrix³¹. Research shows that the reinforced polymer fibers had an increase in tensile modulus and tensile strength increased. Therefore, it may be possible to tailor the mechanical properties of nanofiber scaffolds to resemble that of the target tissue³⁷.

2.9.2 Co-polymer scaffolds

Also, chitosan (nano)-fibers can be created using electrospinning with a chitosan blend and another polymer. Many examples of chitosan blend fibers made through electrospinning have been reported in the literature⁵. Commonly reported blends include chitosan with Poly(ethylene oxide) (PEO) and Ultrahigh-

molecular weight poly(ethylene oxide) (UHMWPEO) . These blends have been found to promote the attachment of human cells while maintaining their shape and health. Other polymers such as Poly(vinyl alcohol) (PVA), Poly(ethylene terephthalate) (PET), Poly(vinyl pyrrolidone) (PVP), and Poly(lactic acid) (PLA) have also been used to form chitosan (nano)fibers. UHMWPEO added to chitosan allows for the formation of fibers ranging from less than a hundred nanometers to a few tens of micrometers, while PVP decreases the diameter of chitosan-based fibers. Chitosan/PVA nanofibers are commonly used for various biomedical applications since they are biocompatible and free of beaded defects. Chitosan/PET nanofibers are also a possible option.

2.9.3 Commercial chitosan products

Chitosan can be derived from various sources, but the most commonly used one is waste crustacean shells, like those of crabs or shrimp, which are obtained from the seafood processing industry. Although there are other potential sources, these are currently not being actively investigated on a commercial basis. There are several chitosan-based products available commercially on the world market. These products come in various forms and are used in different ways in biomedical practice.

For instance, some are used as wound dressings like Hem-Con® Bandage, ChitoGauze® PRO, ChitoFlex® PRO, ChitoSam™, Syvek-Patch®, Chitopack C® and Chitopack S®, Chitodine®, ChitosanSkin®, TraumaStat®, TraumaDEX®, and Celox™. Others are used as hemostatic sealants like ChitoSeat™, while others like Reaxon® (Medovent, Germany) are used as chitosan-based nerve conduits. Reaxon® is resistant to destruction, prevents irritation, inflammation, and infection, inhibits scar tissue and neuroma formation. Chitosan-based nutritional supplements like Epakitin™ and Nutri + Gen® are also available commercially for use in chronic kidney disease in pets. Additionally, various chitosan-based products like ChitoClear®, Chitoseen™-F, and MicroChitosan NutriCology® are sold as safe weight loss supplements, cholesterol-reducing agents, and antioxidant agents¹⁶.

Chapter 3

Methodology

The methodology applied in the present study is summarized in the flow diagram in Figure 3.1. Chitosan of different types and solvents of different nature were used. . The process involves preparing the polymeric solution, processing it through electrospinning, and characterizing the resulting fibers. If no fibers were obtained, new solutions were made by adjusting variables such as the solvent or type of chitosan used. The process of synthesizing fiber was divided into two parts, as illustrated in Figure 3.2. The first part involved determining the optimal conditions for the polymeric solution, while the second part involved identifying the best processing parameters for the electrospinning process. Details of solution preparation and electrospinning processing parameters are explained throughout this chapter.

3.1 Materials

This study used three types of chitosan sources: 1) chitosan from shrimp shells, with a Degree of Deacetylation (DD) of 75–85% and 50 – 190 Kilodalton (kDa) purchased from Ecuachitosan, an artisan manufacturing company, 2) chitosan from crab shells, with a DD of $\leq 85\%$ and 190 – 375 kDa purchased from Ecuachitosan , and 3) commercial chitosan, with a DD of $\geq 75\%$ and 310 - 375 kDa purchased from Sigma-Aldrich. Multiple solvents were utilized in this research, Acetic Acid (AcOH), Trifluoroacetic

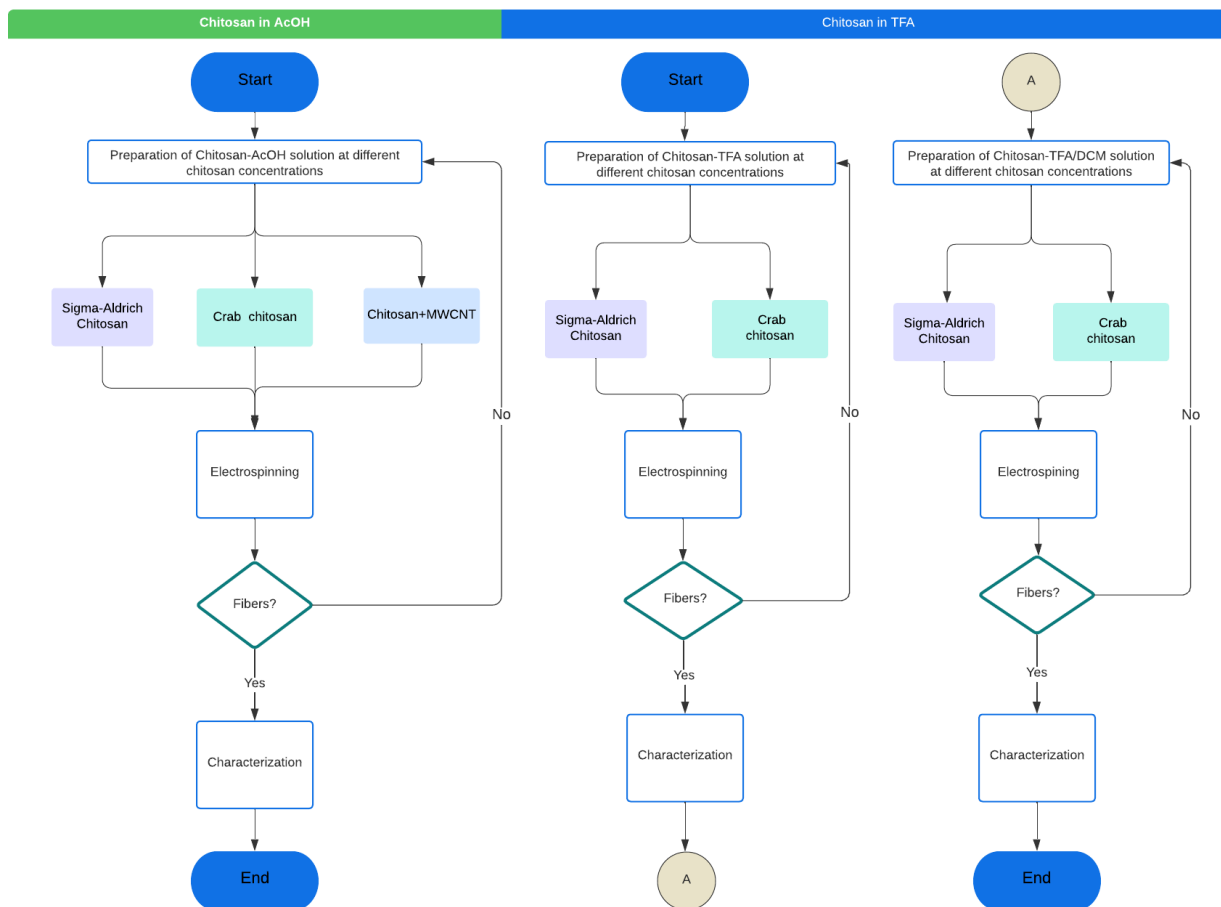


Figure 3.1: Experimentation flowchart

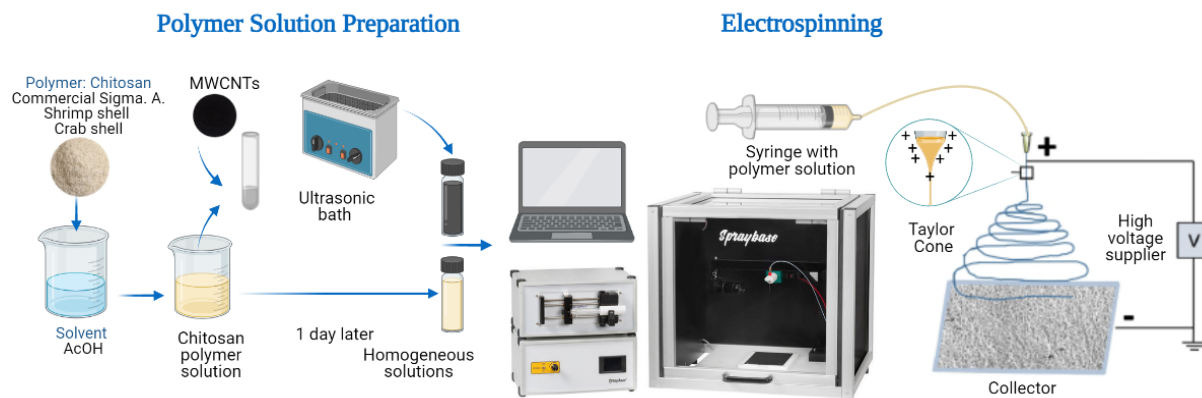


Figure 3.2: Illustration of the fiber synthesis process carried out by electrospinning.

acid (TFA), and Dichloromethane (DCM), acquired from Sigma-Aldrich (USA). These solvents were used directly without any additional purification. The physics department of Yachay Tech University supplied the Multi Walled Carbon Nanotubes (MWCNTs) for usage.

3.2 Electrospinning solution

In the production of fibers, the first step involves creating a polymeric solution, as shown in the first part of Figure 3.2. This study prepared both pure chitosan solutions of different types and solutions of chitosan mixed with MWCNTs to enhance their conductive properties. Also, chitosan was dissolved in various solvent systems, including AcOH, TFA, and DCM, which are used in solution dynamic studies of chitosan. Detailed information about the solvent, chitosan type, and polymer concentration used in preparing the samples can be found in Tables 3.1, and 3.2. All samples were prepared under a biosafety cabinet at room temperature.

Solvent	Polymer	Chitosan Concentration % (w/v)
AcOH	Commercial Chitosan	2
		2,5
		3
	Shrimp Chitosan	6
		7
		8
	Crab Chitosan	3
		4
		5
	Commercial Chitosan+MWCNT	2
		2,5
		3
	Shrimp Chitosan+MWCNT	6
		7
		8
Crab Chitosan+MWCNT	3	
	4	
	5	

Table 3.1: Chitosan samples using AcOH as solvent

Solvent	Polymer	Chitosan Concentration % (w/v)
TFA	Commercial Chitosan	2
		2,5
		3
	Crab Chitosan	3
		4
		5
TFA/DCM	Sigma-Aldrich	3
		4
		5
	Crab Chitosan	3
		4
		5

Table 3.2: Chitosan samples using TFA and DCM as solvent.

3.2.1 Chitosan in AcOH

Chitosan can dissolve in both acidic and alkaline solutions. In this investigation, acetic acid is the preferred solubilization agent due to its widespread use for this purpose. In order to make the chitosan solution, it's important to first prepare a mixture of acetic acid and distilled water. This study utilized a 3% (v/v) AcOH solution as a solvent. Then, a specific amount of chitosan is weighed on an electronic balance and added to a AcOH solution to test for different concentrations. The amount of chitosan used is determined by the desired percentage concentration (x%). In this work, the polymer solution is prepared with the different types of chitosan at different concentrations to find the most suitable ones for the electrospinning process. To prevent degradation of the chitosan, the solution was prepared at room temperature. After mixing, it should be left in a dark place until it becomes homogeneous, ideally for 24 hours, to prevent lump formation.

3.2.2 Chitosan +MWCNT in AcOH

Solutions were prepared with the three types of chitosan mixed with MWCNTs at a concentration of 0.3% by chitosan weight as reported Bahadır³⁸. MWCNTs has conductive properties that improve the electrospinning ability of the solution. As a first step, chitosan solutions dissolved in AcOH were prepared at the same concentrations as the procedure described in section 3.2.1. Then the MWCNTs were added to the homogeneous solution. The solution was subjected to an ultrasonic bath for 90 minutes to mix the MWCNTs in the chitosan solution completely. The chitosan+MWCNTs solution was stored at room temperature in a dry place for further processing by electrospinning.

3.2.3 Chitosan in TFA and TFA/DCM

The solvent was changed to TFA and new samples were prepared by mixing the chitosan powder in TFA (99% purity). Then a 70:30 TFA/DCM cosolvent was prepared as proposed by Ohkawa³⁹. New samples were prepared by mixing the chitosan powder in the TFA/DCM cosolvent. The solutions were stored in a dark place for 24 hours until homogeneous, then they were processed in electrospinning.

3.3 Electrospinning

Electrospinning unit at Yachay Tech is a Spraybase® Electrospinning Starter Kit which is composed of syringe pump, 20kV Power Supply Controller and collector (see Figure 3.3). The processing parameters such as can needle diameter, collection distance, flow rate and voltaje used in this study can be found in the Appendix A.

The procedure used in this study to process the samples by electrospinning is detailed in Table 3.3 . The solution was poured into a 10 mL syringe attached to a stainless steel needle via standard polyvinylidene fluoride tubing. The syringe was then inserted into a programmable syringe pump. Then, a suitable pumping speed was set, ranging between 0.05 to 0.1 mL/Hr. The aluminum foil as a collector was placed 6-15 cm from the end of the syringe. High voltage DC power was delivered to the syringe and gradually increased until a stable jet was attained. After every experiment, the high-voltage power supply was turned off, and a new layer of aluminum foil was laid on the collector. The power was turned on, and samples were collected for 1 hour for each experiment. Each solution was tested under ambient conditions. To ensure similar conditions, the temperature and humidity levels were noted for each experiment, and the ambient temperatures were within (17 ± 2) °C, and relative humidity levels were within (60 ± 3) % of each process run. Each sample was appropriately stored after ensuring adequate drying of the fibers.

3.4 Characterization

Biomaterial characterization combines theoretical and experimental methods and successive experimental testing. Existing experimental instrumental techniques for the characterization of biomaterials could be divided into methods for the characterization of spatial structure, measurement of surface characteristics, and determination of the composition and structure of biomaterials, phase transformations, and molecular weight distribution³¹. Surface properties occupy a central place in biomaterial characterization since there is a correlation with the biological performances of biomaterials.

Steps	Procedure
1	Make sure the voltage generator and the programmable syringe pump are off.
2	Fill up the syringe with chitosan solution.
3	Attach the syringe to the PVDF tube.
4	Wait for all air bubbles to dissipate from the solution.
5	Place the syringe in the programmable syringe pump.
6	Set the desired flow rate in mL/Hr.
7	With the help of the motion controller, the distance between the needle tip to the collector is adjusted
8	Make sure the voltage supply wire is connected to the needle of the syringe.
9	Set up the aluminum foil on the collector.
10	Align the needle in such a manner that it is in the center of the collector.
11	Turn on the voltage generator.
12	Change flow rate to the desired flow rate.
13	Adjust the voltage
14	If the pendant drop dries out at the needle tip, turn off the voltage generator before cleaning capillary tip.
15	After collecting fibers, zero the voltage indicator, the turn off the voltage generator.
16	Discard the PVDF tube and clean the valve and collector properly.

Table 3.3: Step-by-step procedure for operating electrospinning.

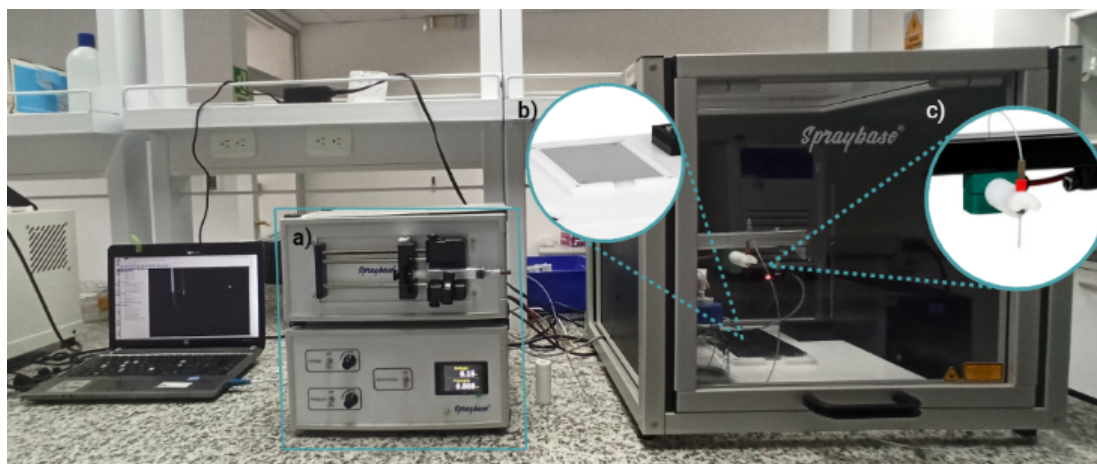


Figure 3.3: Electrospinning unit at Yachay Tech University: a) high voltage supply , b) collector, and c) syringe pump.

3.4.1 Scanning Electron Microscopy (SEM)

Scanning electron microscopy (SEM) is an essential tool capable of producing high-resolution images of a sample surface. SEM measurements were conducted on a field emission scanning electron microscope. This microscope generates images of a sample by examining it with a focused beam of electrons. The electrons interact with atoms in the specimen, producing various signals that can be discovered and that comprise data about the sample surface topography and composition. SEM can attain a resolution better than 1 nanometer. Once the samples were dry, the morphology and diameter of the electrospun nanofibers can be observed by using field emission SEM.

In this study, SEM characterization was made using JEOL JSM-IT300 at an accelerating voltage of 15kV. An illustration of the SEM equipment used in this study is shown in Figure 3.5. Samples were cut from electrospun mats on an aluminum foil and mounted on metal stubs using double-sided carbon tape. Before observation, the samples were coated for 3 min with gold using the plasma sputtering (108C Auto/SE Carbon Coater sputtering Figure 3.6) to prevent charging in the SEM electron beam. See Figure

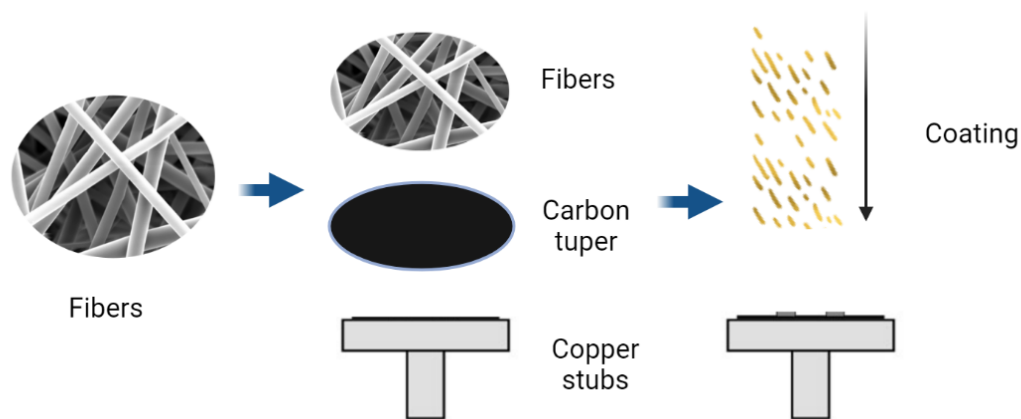


Figure 3.4: Fiber sample preparation for SEM

3.4 for a schematic of sample preparation for SEM. Diameters and distribution evaluation of the electrospun nanofibers were analyzed from the SEM images by using ImageJ analysis software. For each electrospun mat, several fibers were considered from different locations on the sample to calculate the average fiber diameter.

ImageJ software was used for the analysis of the SEM micrographs. ImageJ was developed by the U.S. National Institutes of Health. ImageJ is in the public domain and runs on any operating system. It has found wide usage in many research areas, including nanotechnology. ImageJ is used to determine the diameter of the nanofibers at every pixel along the fiber axis. Various software is available to measure items of the image manually using scale bar calibration.

3.4.2 Raman spectroscopy

Raman Spectroscopy is a method of analysis that allows for examining a material's chemical properties and vibrational modes without causing damage. It also provides information about materials' structure,



Figure 3.5: Scanning Electron Microscopy (SEM) illustration



Figure 3.6: 108C Auto/SE Carbon Coater. Equipment used for sample coating prior to SEM characterization.

phase, and crystallinity. This method is commonly used to identify the vibrational modes of molecules, including pyranoid ring, in-plane or out-plane bending, and stretching vibrations. Raman scattering represents a high-resolution spectroscopic technique based on the interaction of Infrared radiation with the vibrational modes of the examined molecular system. This vibrational technique helps us map a surface and get a chemical characterization at every sample point. Raman scattering vibrational spectrum provides similar but complementary information to Infrared radiation spectroscopy. This method enables the determination of the spatial structure of electron density distribution and electronic-vibrational interaction in biomolecules, biomaterials, and in the sub-molecular condensed state.

Vibrational spectroscopy is one of the most important methods covering infrared, near-infrared, and Raman spectroscopies. It is based on the measurement of vibrational energy levels, which are associated with the chemical bonds in the sample. So, the obtained spectra could be used to assess the close intermolecular interactions of specific groups. The spectra obtained by scattering and absorption infrared light provide vibrational data from solid-state or gas-phase samples. Raman vibrational spectroscopic tech-

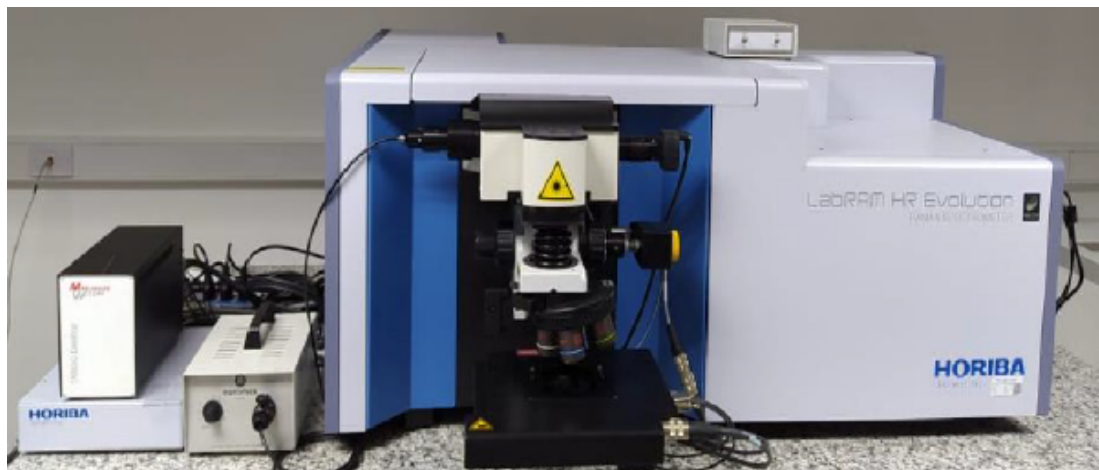


Figure 3.7: Raman spectra were carried out by LabRAM HR Evolution microscope. The excitation laser wavelength was 785 nm.

nique, is of particular significance in providing information about the molecular composition, structure, and interactions within a sample.

The Raman spectroscopy analysis for all our chitosan samples was carried out using LabRam HR Evolution microscope (see Figure 3.7). The following measuring parameters were applied: range – 20 to 3200 cm^{-1} , source of radiation – 785 nm. The Raman spectra were then acquired using an accumulation time of 15 s and summing up 8 accumulations.

Chapter 4

Results & Discussion

Section 4.1 analyzes the numerous factors that affect the electrospinning process of the chitosan polymer solution. These factors comprise the material's molecular weight, solvent nature, boiling point and dielectric constant. Section 4.2 describes the morphology through Scanning electron microscopy (SEM) spectroscopy of fibers obtained from the improved procedures of section 4.1. The morphology varies from beaded fibers to fibers without beads, depending on the specific materials/processing parameters. Finally, section 4.3 shows Raman characterization of the fibers obtained in the present investigation.

4.1 Optimising the polymer solutions and process parameters in the electrospinning of chitosan

Understanding electrospinning can be challenging due to the interplay between the electric field and fluid deformation, which is determined by the material's rheology. This section examines several factors, including the properties of the solution, processing, and solvent nature, that impact the conversion of polymer solutions into electrospun fibers. Regulating these parameters is essential to ensure the electrospun fibers'

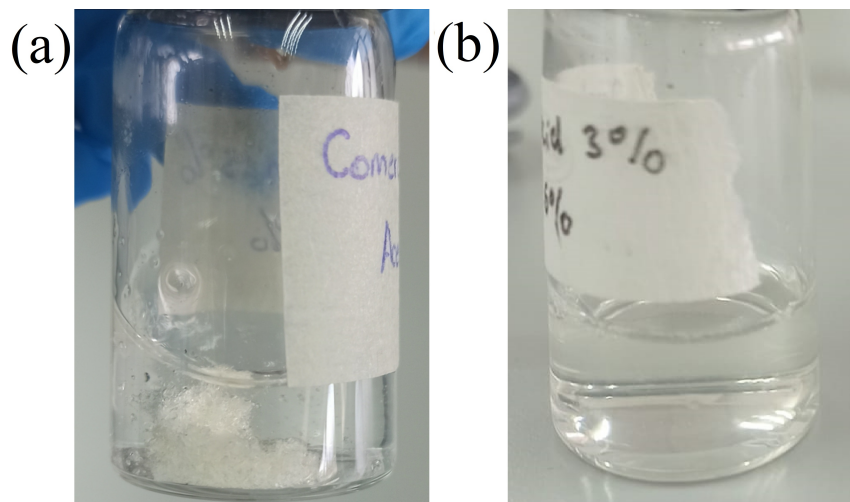


Figure 4.1: Comparison of the chitosan solution before mixing and after several hours of mixing when homogeneity was achieved.(a) Solution with chitosan lumps (b)Homogeneous solution.

desired morphology and chemical structure.

In this study, it was found that samples of shrimp chitosan, crab chitosan and commercial chitosan dissolved well in Acetic Acid (AcOH) as a solvent. All three types of chitosan examined showed great solubility, and the solutions were uniform regardless of polymer concentration. A solution is considered homogeneous when it is completely dissolved without any visible lumps, as shown in Figure 4.1.

The mechanism of chitosan dissolution in AcOH can be resumed in Figure 4.2. This reaction results in the protonation of the NH_2 group of chitosan and is responsible for the dissolution of chitosan in aqueous acetic acid medium. The solubility of chitosan is attributed to the presence of amine groups in its structure, which are protonated in acid media, resulting in positive charges distributed along their chains NH_3^{+40} . Protonation of the amino groups is a necessary step to dissolve chitosan powder in aqueous medium.

It is evident from Figure 4.3, that there are differences in the time it takes for dissolution among the

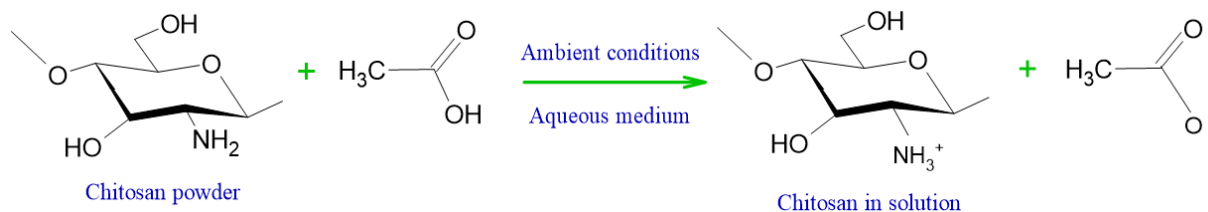


Figure 4.2: Chemical reaction of chitosan dissolved in AcOH. Chitosan was protonated in AcOH and form polycation chitosan.

different types of chitosan. The time to obtain a homogeneous solution increases as the concentration of chitosan in the solution increases, Chitosan obtained from Sigma Aldrich and crab shells dissolve slowly because of their high Molecular Weight (MW). In contrast, the chitosan extracted from shrimp shells has a low MW, which makes it dissolve faster. Based on existing literature³⁵, it is evident that the solubility of chitosan is influenced by its MW. Viscosity of chitosan increases with increase in its MW and concentration. Specifically, the higher the MW of chitosan, the greater the number of hydrogen bonds formed in its polymer chain, resulting in a more complex dissolution process⁴¹. The solution only attained homogeneity after the complete dissolution of chitosan powder without any visible lumps in the solvent.

Different chitosan samples were processed at different concentrations, but no fibers were obtained. Although different types of chitosan of different MW were tried, it was not possible to obtain pure chitosan fibers using AcOH as solvent. The solution is unsuitable for electrospinning as the Taylor cone cannot be formed. Therefore, in order to improve the conductive properties of the solutions, new solutions reinforced with Multi Walled Carbon Nanotubes (MWCNTs) were prepared. With the chitosan/MWCNTs composite, the electrospinning process becomes more stable. The chitosan/MWCNTs solutions showed good nanotube dispersion as shown in Figure 4.4.

However, it is not possible to observe the formation of fibers using Chitosan/MWCNTs composite as shown in Figure 4.5. When pure chitosan and MWCNTs-reinforced chitosan samples were dissolved in

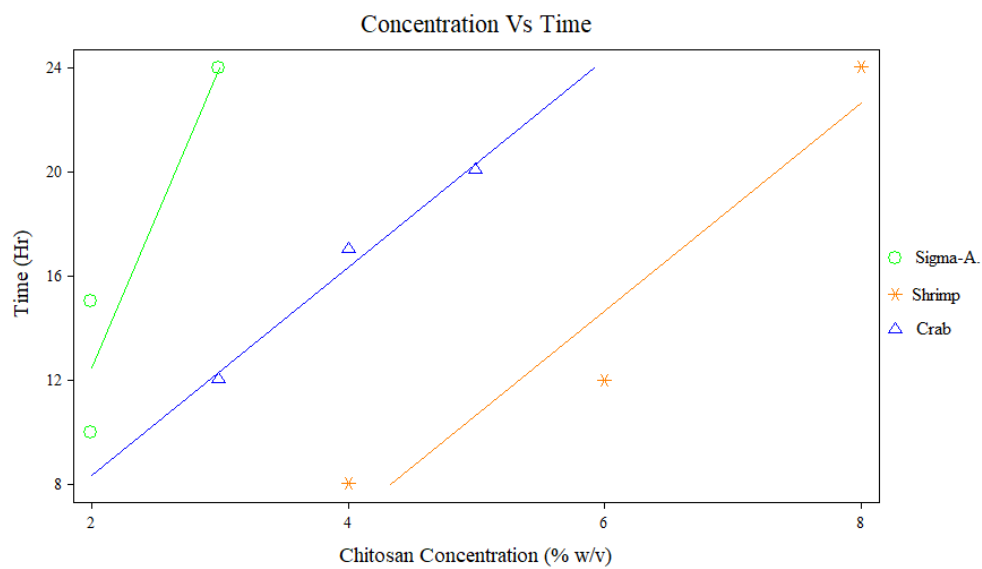


Figure 4.3: Time for chitosan to dissolve in AcOH

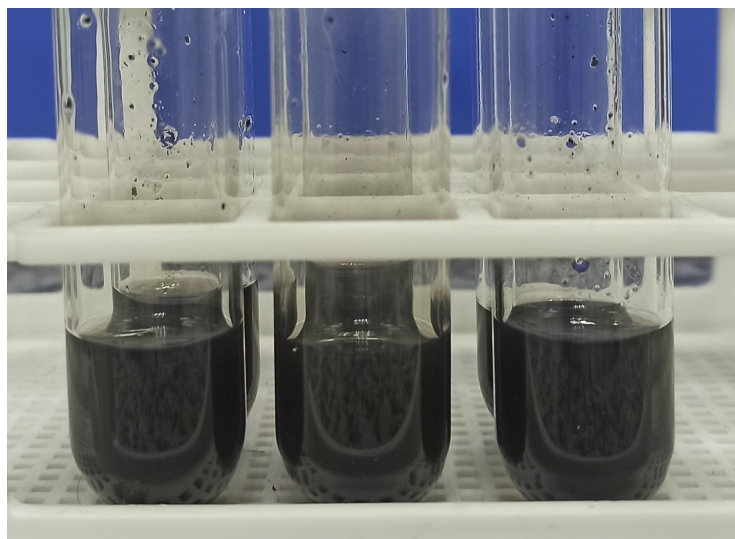


Figure 4.4: MWCNT-reinforced chitosan samples

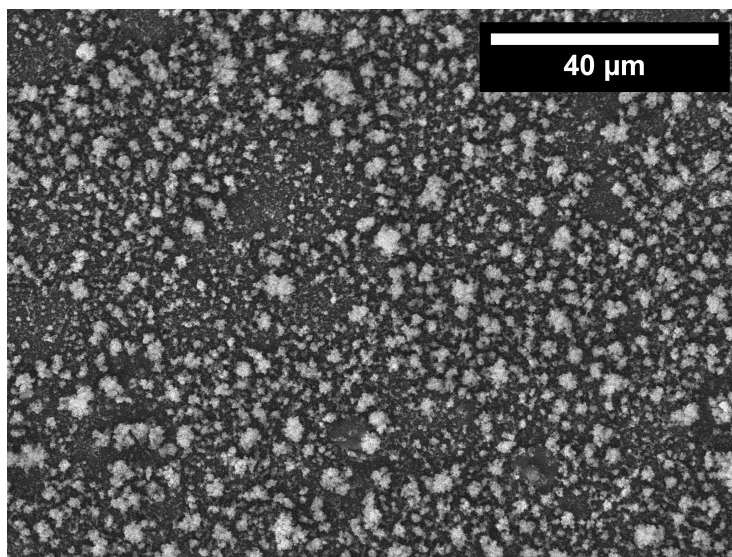


Figure 4.5: SEM photograph of the deposited chitosan using AcOH as solvent.

AcOH as a solvent and subjected to high voltagee even above 18kV, no steady jet was produced during the electrospinning process. As a result, it was not possible to obtain electrospun chitosan fibers using these conditions.

The tests conducted revealed that obtaining fibers with AcOH as solvent is not feasible despite testing different concentrations of chitosan with varying molecular weights. AcOH by itself is incapable of reducing the surface tension of the polymer drop in the electrospinning process³⁴. This behavior can be attributed to the high boiling point exhibited by the AcOH solutions, does not allow it to evaporate quickly from the jet surface of the polymer solution when voltage is applied⁴². Table 4.1 shows information on the solvents used in this study. The boiling point is related to the evaporation rate of the solvent and the dielectric constant represents the amount of free charge that can be induced into the polymer solution during electrospinning⁴³. Generally, a solvent with a higher dielectric constant encourages solvent evaporation and reduces bead formation, resulting in the formation of fibers with lower average diameter⁴⁴.

System	Dielectric constant	Boiling point (°C)
TFA	39.0	71.8
DCM	9.1	39.8
TFA-DCM 7:3	29.0	61.1
Acetic acid	6.2	118.1
Water	78.5	100.0

Table 4.1: Dielectric constant and boiling point of the solvents

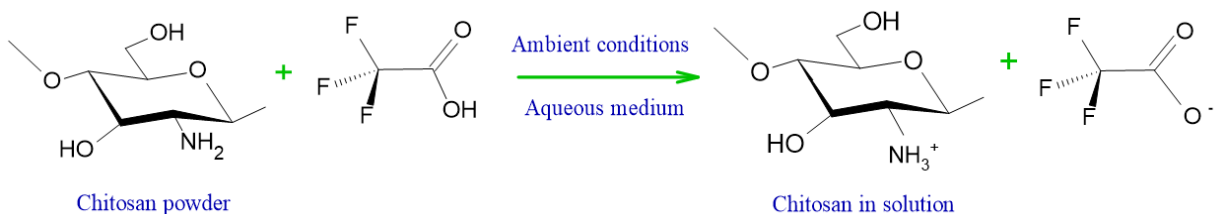


Figure 4.6: The chemical reaction between chitosan and TFA

Electrospinning of pure chitosan from weak acids (AcOH), more commonly used for dissolving chitosan, was found to be a real challenge as previously reported in this research. In the best cases, only nanobeads were formed. A similar study suggests that for this reason, a strong acid, with a low boiling point and high dielectric constant, namely i.e. Trifluoroacetic acid (TFA), was utilized³⁹. Figure 4.6 shows the possible reaction that occurs when dissolving chitosan in TFA. In this reaction, the amino groups of the chitosan can form salts with TFA, which can effectively destroy the intermolecular interactions between the chitosan molecules and thus facilitate electrospinning⁴⁵.

It was only possible to obtain fibers by changing the solvent to TFA, being the 2.5% w/v commercial chitosan sample the one that showed the best results. Electrospinning TFA fibers can be achieved for two reasons. Firstly, the solvent creates salts with the amino groups in chitosan, which breaks down the rigid

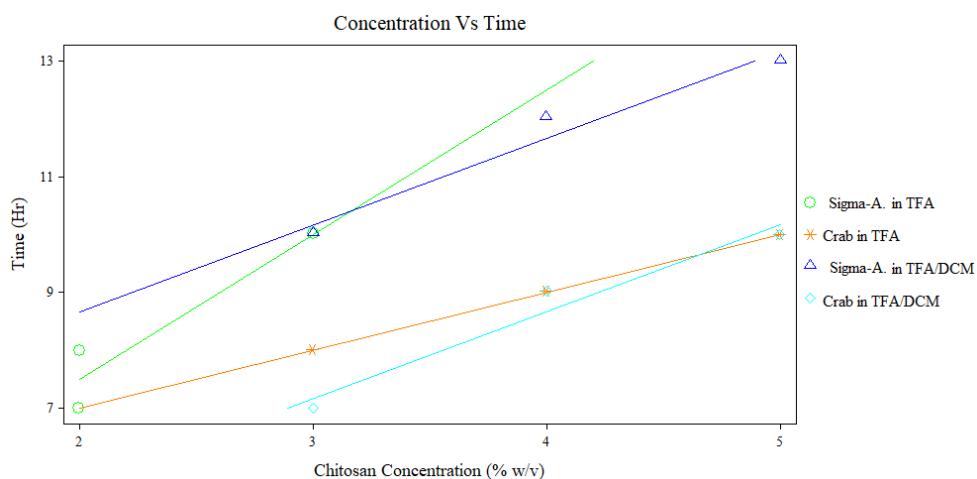


Figure 4.7: Time for chitosan to dissolve in TFA and TFA/DCM

interaction between chitosan molecules and makes it suitable for electrospinning²⁵. Secondly, the solvent has a high volatility, which causes the electrospinning process to solidify into visible fibers in the collector quickly¹. Figure 4.7 provides the specifics of the amount of time it takes for the chitosan-TFA solution to become homogeneous. The time it takes for chitosan to dissolve in TFA until it becomes a uniform solution is directly related to its MW. The greater the MW, the longer it takes to dissolve. This finding is similar to the results obtained from the chitosan dissolution process in AcOH.

Although it was possible to obtain fibers using the TFA system, this system still produced beads and droplets. This was due to the high repulsive interaction between the poly-cations along the chitosan chains, which prevented the formation of sufficient chain entanglements required for proper fiber formation¹⁷. The literature suggests that the best solvent system for electrospinning chitosan solutions is TFA-Dichloromethane (DCM) (TFA-DCM)^{33,46}. The study examined how electric field strength, solvent ratio, and chitosan concentration affect the diameter of fibers. Results showed that using 13kV-17kV, TFA/DCM solvent ratio of 70/30% v/v, and a 4% w/v chitosan concentration produced the most uniform fibers. The experiment used Sigma-Aldrich commercial chitosan and crab chitosan at this concentration. Table 4.2

provides more information on the processing parameters used to achieve fiber production.

Sample	Polymer Concentration (w/v) %	Needle diameter (mm)	Collection Distance (cm)	Flow rate (mL/Hr)	Voltage (kV)	Result
Sigma-Aldrich in TFA	2,5	0,7	10	0,1	14	Fibers with beads
Sigma-Aldrich in TFA/DCM 70/30	4	0,9	12	0,05	13	Bead-free fibers
Crab Chitosan in TFA/DCM 70/30	4	0,9	12	0,05	17	Bead-free fibers

Table 4.2: Processing parameters of chitosan samples with better electrospun fiber performance.

Figure 4.8 compares the droplet when the polymer is dissolved in AcOH (a) and when it is dissolved in TFA (b). In (a) The solution presents a high surface tension which does not allow the drop to form a stable Taylor cone in the electrospinning process. In this case, the electrical energy inside the drop is greater than that created by electrospinning, so it is not possible to form a stable jet to make fibers¹³. While in (b) TFA creates the necessary instability in the system for the Taylor cone to form. In this case, the electrostatic repulsion between charges on the jet surface tends to increase the surface area and thus favors the formation of a thin jet associated to the electrospinning process

In general, it is accepted that the formation of beads can be eliminated if the influence of the surface tension is suppressed⁴⁷. Due to the dielectric constant and boiling point of DCM being a lot lower than those of water, its presence in the solvent system increased the rate of evaporation of the solvent, which reduced the very strong charge density contributed by TFA, thus resulting in ultrafine fibres .

To ensure successful fiber processing, it is crucial to maintain a voltage range between 13kV-17kV. Going beyond the 20kV limit will result in the formation of two Taylor cones in the electrospinning jet,

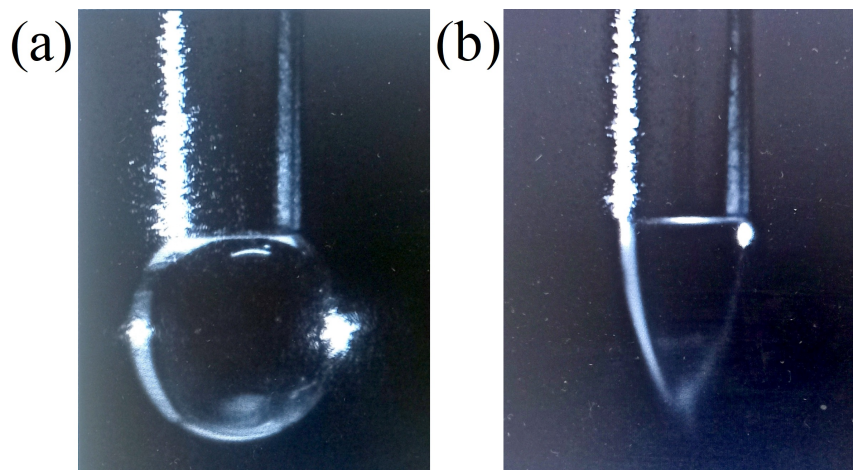


Figure 4.8: Drop of polymer solution in the process of electrospinning (a) using AcOH (b) using TFA

which will impede the production of continuous fibers due to the excessively high voltage. Moreover, if the distance between the collector and needle is less than 6cm, the elongation of the polymer jet will be hindered, leading to a repulsion phenomenon, which is illustrated in Figure 4.9. In cases where the polymer concentration in the solution is too high (5 % w/v), the droplets dry out at the needle tip before the polymer jets can be initiated, which ultimately prevents electrospinning³².

The results show that the polymer concentration factor in electrospinning is not only affected by the MW of the polymer used but also by the interactions between polymer and solvent. The properties of the polymer solution, such as its rheological and electrical properties, are greatly influenced by the nature of the solvent and the MW of the polymer.

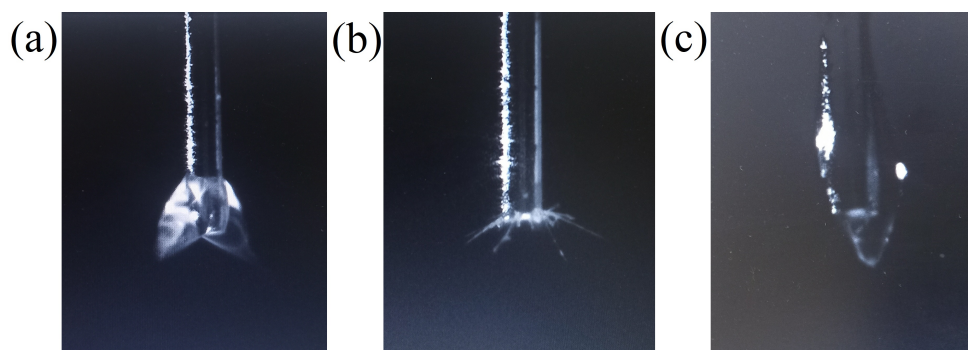


Figure 4.9: Shape of the polymer solution jet at different processing parameters. Chitosan in TFA solution.
(a) High voltage (b) Short distance between the needle and the collector (c) Too concentrated solutions

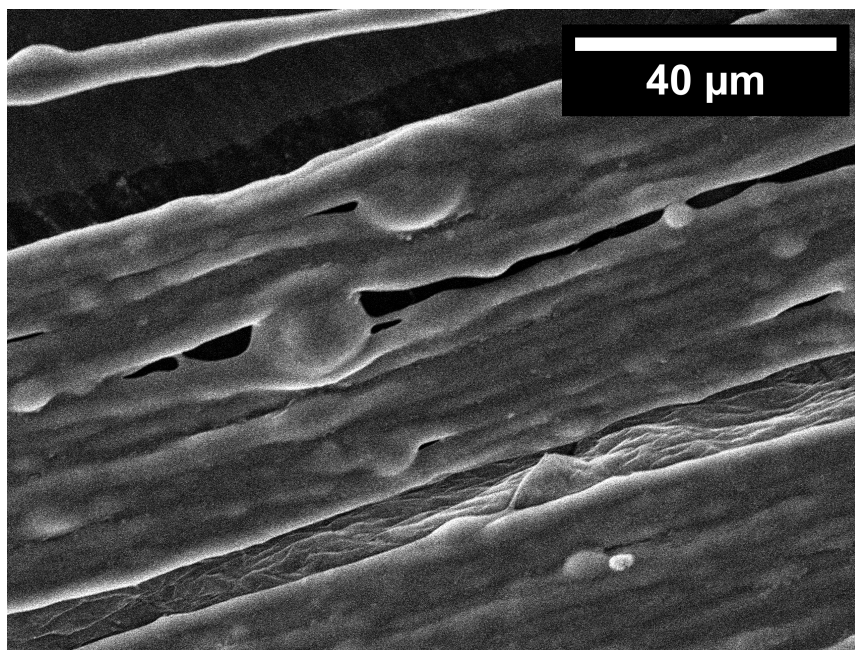


Figure 4.10: SEM image Electrospun Sigma-Aldrich Chitosan 2,4 % (w/v) TFA (magnification x 1,000)

4.2 Scanning Electron Microscopy

Upon successful completion of the electrospinning procedure, a thorough examination of the fiber structure within the collected membranes was conducted. Regardless of the nature of the chitosan, only when TFA is used as a solvent can fibers be obtained. Figure 4.10 shows the best result that could be obtained using only TFA as a solvent, beads are observed in the fibers. The fibers were made with Sigma Aldrich commercial chitosan at 2.5% w/v chitosan in the solution, showing a diameters ranging from 4.7 to 7.33 μm .

Bead-free fibers were obtained using Sigma-Aldrich chitosan and crab chitosan both at 4% w/v polymer concentration using TFA/DCM as solvent. The application of co-solvent in chitosan with a volumen ratio TFA:DCM 70:30 led to a successful electrospinning experience, altogether avoiding the electrospaying phenomenon, as shown in Figure 4.11 and 4.12.

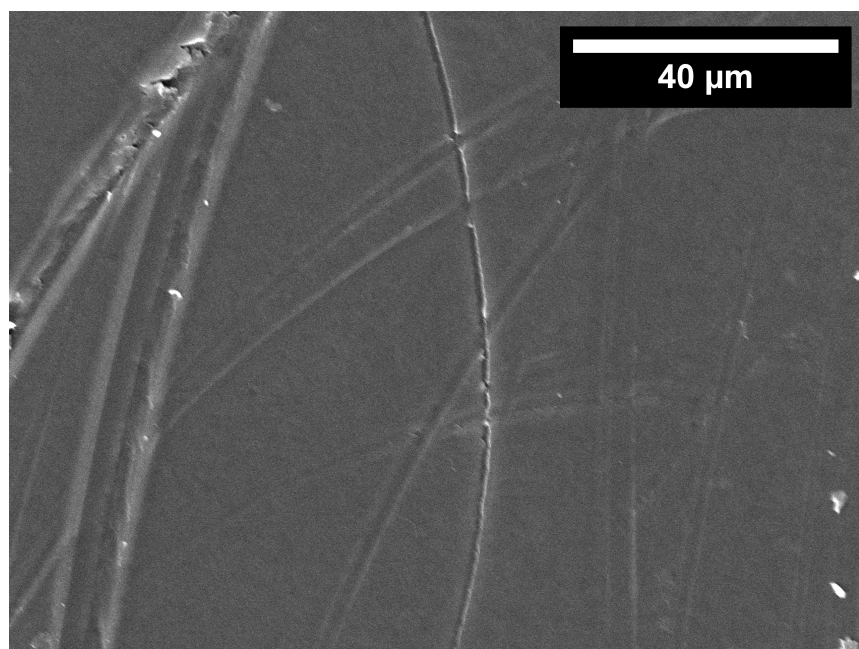


Figure 4.11: Electrospun Sigma-Aldrich Chitosan 4% (w/v) TFA: DCM (magnification x 1,000)

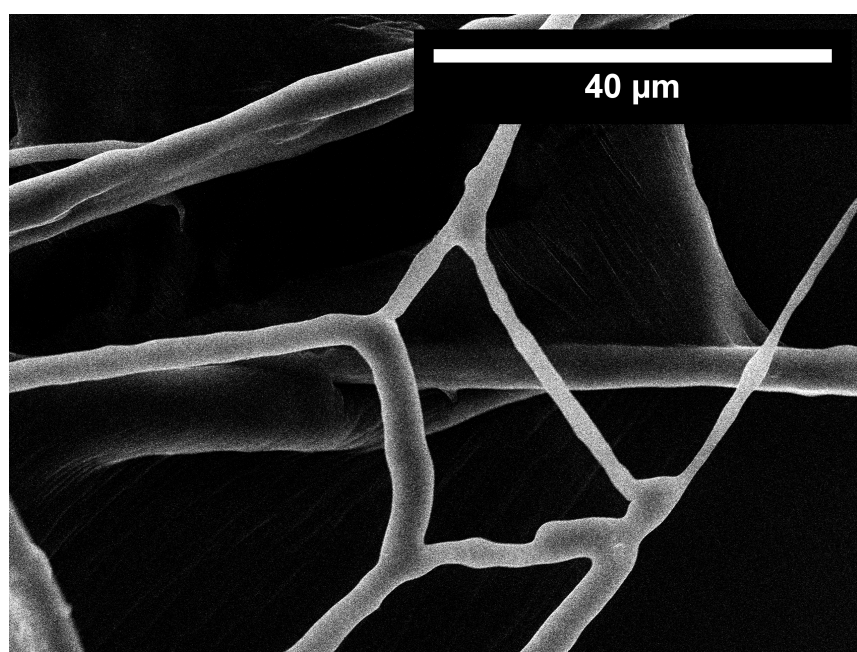


Figure 4.12: Electrospun Crab Chitosan 4% (w/v) TFA: DCM (magnification x 1,500)

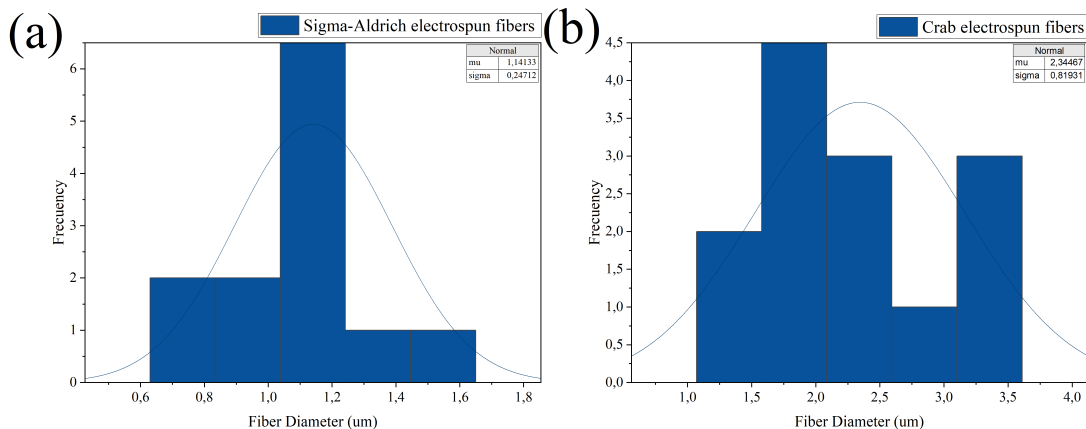


Figure 4.13: Fiber diameter histogram (a)Sigma-Aldrich electrospun fibers (b) Crab electrospun fibers

Figure 4.11 showcases the fibers produced from commercial Sigma-Aldrich chitosan 4% (w/v), which exhibit a structure without beads, indicating that the parameters employed during the electrospinning process were appropriate. The continuous fibers show a random distribution along the membrane and the diameter histogram shown in 4.13 (a) indicates that the average diameter of the fibers is 1.4 um. A selected SEM image of the as-spun chitosan fibrous membranes from crab chitosan is shown in Figure 4.12. Clearly, fibers with smooth and bead-free structure were obtained. These fibers possess a smooth appearance and an average diameter of 2,34 um.

Compared to the fibers made with commercial chitosan in Figure 4.11, the crab chitosan fibers showed an increase in diameter. Since both types of chitosan, shrimp and commercial chitosan, have a high molecular weight, the increase in diameter is due to processing parameters such as voltage. This result is consistent with the literature which indicates that the higher the voltage, the larger the diameter of the resulting fibers⁴⁸.

Using TFA/DCM as a solvent resulted in fibers with smaller diameters than those made with only TFA.

This decrease in diameter is beneficial for biomedical purposes. For example, nanofibrous yarn materials consist of multiple bundles of very fine nanofibers interconnected to form a material structure with high mechanical integrity and are commonly used in the fabrication of various biomedical materials such as sutures⁴⁹. The diameter of fiber using TFA/DCM is strongly affected by the electrospinning conditions as well as by the solvent. Thus, the DCM presence in the solution reduced the extremely strong charge density originated by the TFA and also generated better electrospinnability conditions by reducing even further the boiling point.

Increasing the solution viscosity by increasing the polymer concentration yields uniform fibres, with the formation of fewer beads. Variation in solution viscosity is responsible for many of the morphological changes in fibres. Hence, even when polymer concentration is low, high molecular weight polymer can maintain a sufficient number of entanglements in the polymer chains, to provide an adequate level for solution viscosity.⁵⁰ It is important to note that the best chitosan fiber formation occurred with medium-high MW chitosan, such as commercial chitosan and crab chitosan. This is due to an overall increase in solution viscosity and a decrease in surface tension, as explained above. However, it is crucial to avoid low viscosities that cause droplets to form and high viscosities that lead to flow instability due to the solution's high cohesiveness⁵¹. Consequently, surface tension and viscosity, which are a function of the mass density (concentration and MW) of the polymer in a solvent, play a major role in determining the morphology of the spun material by an electrostatic force. Molecular weight also has a significant effect on the polymer rheological and electrical properties, such as: viscosity, surface tension, conductivity and dielectric strength. It has been observed that a very low MW solution tends to form beads rather than fibres, while higher MW polymer solutions produce fibres with higher average diameter.

4.3 Raman Spectroscopy

Raman spectroscopy can provide reliable evidence of functional chitosan groups through its characteristic peaks, making it a useful tool for structural analysis⁵². When analyzing the Raman spectrum of chitosan, it is common to observe multiple peaks that correspond to different functional group vibrations within the polymer chain. According to the literature²⁴, the prominent Raman peaks of the chitosan spectrum can be assigned as the following; the C-C stretching region (1050-1200 cm^{-1}), Amide-III (1313-1450 cm^{-1}), Amide-II (1550-1600 cm^{-1}), Amide-I (1630-1730 cm^{-1}), and C-H (2888-2897 cm^{-1})⁵³.

As described in section 4.1, only when the solvent is changed to TFA could fibers be obtained by electrospinning. Figure 4.14 shows the Raman spectrum of the fibers made using only TFA as a solvent. It can be seen that the spectrum of the pristine material (chitosan from Sigma-A.) and the spectrum of the fiber are similar, this is due to the fact that in the electrospinning process the solvent evaporates before the fiber is deposited in the collector. In the electrospinning process, there exists a rapid solvent evaporation as well as phase separation as the polymer solution jet is thinned¹⁴. Therefore, the chemical characterization of the fiber shows the spectrum of the pure material. This result also demonstrates that the solvent has the ability to protonate the amine groups of chitosan without compromising its degradation.

The spectrum of the pristine material (Sigma-Aldrich) in Figure 4.14 the peaks 426, 493, 896, 1101, 1264, 1376, 1659 and 2888 cm^{-1} correspond respectively to the out-of plane bending vibration of (OH), the in-plane bending vibrations of(CO-NH₂), the stretching vibration of pyranoid ring, the stretching vibration of (C-O-C), the in-plane bending vibrations of (O-H), vibration of Amide-III and vibration of Amide-I⁵⁴.The fiber spectrum in Figure 4.14 shows a band at 1376 cm^{-1} related to Amide-III, while the second band is a stretching vibration of the pyranoid ring with a low-frequency vibration at 896 cm^{-1} .

The peaks in Figures 4.14, 4.15 and 4.16 that are between the ranges 500 cm^{-1} to 730 cm^{-1} can be associated the interaction between TFA and chitosan molecule which the two possible modes are the symmetric

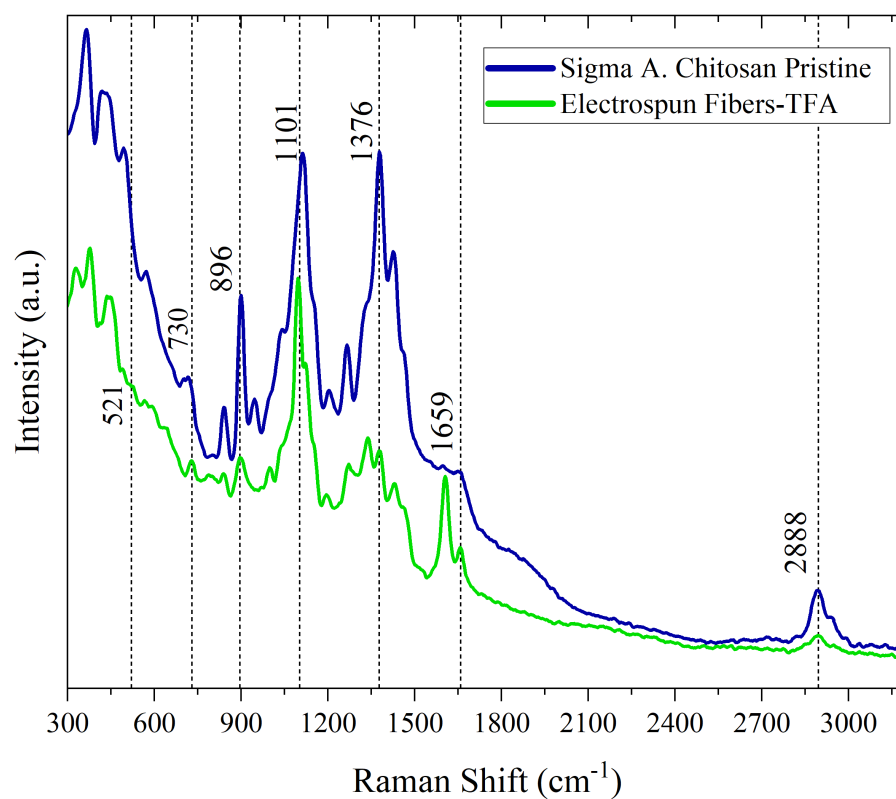


Figure 4.14: Raman spectra of Sigma Aldrich chitosan fibers made by electrospinning using TFA as solvent

CF₃ and CO₂ deformation⁵⁵. CO₂ vibration in the trifluoroacetate ion should be identified with the sharp intense band at 730 cm^{-1} . The symmetric CF₃ deformation mode has been assigned a value between 500 and 700 cm^{-1} . In this investigation, we cannot relate the presence of TFA to the CO₂ vibration at 730 cm^{-1} because this band is also associated with the chitosan molecule, as shown in Figure 4.14. The band at 730 cm^{-1} shows a peak in the pristine chitosan material, so to identify the presence of TFA in the fibers, we discard the band at the 730 cm^{-1} level and use the band range of 500- 700 cm^{-1} . The sharp moderately intense band at 601 cm^{-1} is attributed to the CO₂ deformation in the trifluoroacetate ion⁵⁶. A remarkable fact is that the signatures related to the CF₃ group (601 and 521 cm^{-1}) were not clearly observed in the Raman spectra of the fibers made by electrospinning indicating little or no presence of the solvent in the resulting fibers.

In the sample Sigma-Aldrich chitosan TFA/DCM Figure 4.15, Raman signatures related to the amide groups of chitosan molecule were noted at 1378 and 1659 cm^{-1} . The characteristic functional groups of chitosan found in the fiber spectrum using Sigma Aldrich chitosan are described in more detail in Table 4.3.

Figures 4.15 and 4.16 show a similarity between the spectrum of the resulting fiber and the spectrum of the pristine material when the cosolvent is used (TFA:DCM). This result is similar to that found when only TFA is used as solvent. The Raman spectra of the 3 samples measured displayed small variations in the intensities in the 1200–1300 cm^{-1} region. These variations are mainly attributed to the vibration of the C-H group⁵⁵,

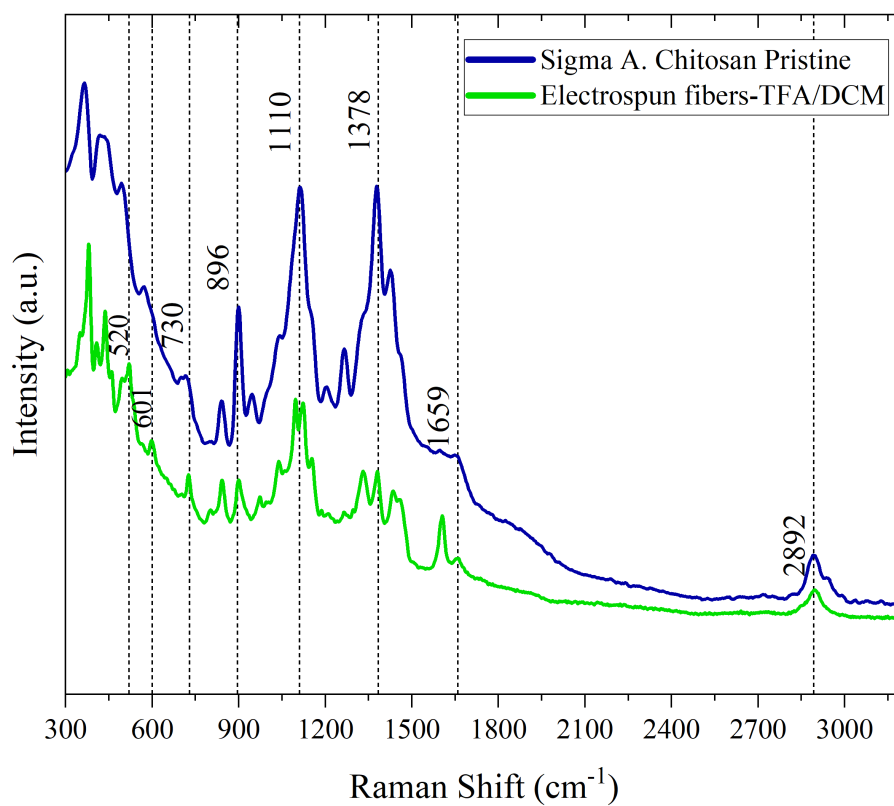


Figure 4.15: Raman spectra of Sigma Aldrich chitosan fibers made by electrospinning using TFA:DCM as solvent

Pristine Chitosan		Electrospun fibers		Bands assignment
Sigma-A.	Crab	TFA:DCM Sigma-A.	TFA:DCM Crab	
2892	2897	2892	2897	$\nu(\text{CH}_2)$
1659	-	1659	-	Amide-I
1378	1382	1378	1382	Amide-III
1264	1256	1264	1263	$\delta(\text{OH}\dots\text{O}) + \nu(\text{C-C}) + \nu(\text{C-O}) + \delta(\text{OH}) + \rho(\text{CH}_2)$
1110	1101	1118	1101	$\nu(\text{C-O-C}) + \nu(\phi) + \nu(\text{C-OH}) + \nu(\text{C-NH}_2) + \delta(\text{CH}) + \rho(\text{CH}_2) + \rho(\text{CH}_3)$
1044	1038	1040	1030	$\rho(\text{CO}_3) + \delta(\text{CH}) + \delta(\text{OH})$
-	998	-	979	$\nu(\phi) + \rho(\text{CH}_2)$
943	941	-	-	$\nu(\text{CN})$
896	897	898	897	$\nu(\phi) + \rho(\text{CO-NH}_2)$
730	709	730	-	$\nu(\text{CO}_2)$
-	-	601	-	$\nu(\text{CF}_3)$
-	-	521	-	$\nu(\text{CF}_3)$
493	493	493	486	$\delta(\text{CO-NH}_2)$
426	421	433	421	$\gamma(\text{OH}) + \gamma(\phi)$
363	357	377	357	$\gamma(\text{OH}) + \gamma(\phi)$

Table 4.3: Wavenumbers of the bands observed in Raman spectra for Pristine Chitosan Sigma-Aldrich (CS S.A), Chitosan TFA:DCM Sigma-Aldrich Fiber (CS TFA:DCM S.A Fiber), Pristine Chitosan Crab (CS Crab), Chitosan TFA:DCM Crab Fiber. ϕ -pyranoid ring, ν - stretching, δ - bending in plane, γ and ω -bending out-of plane.

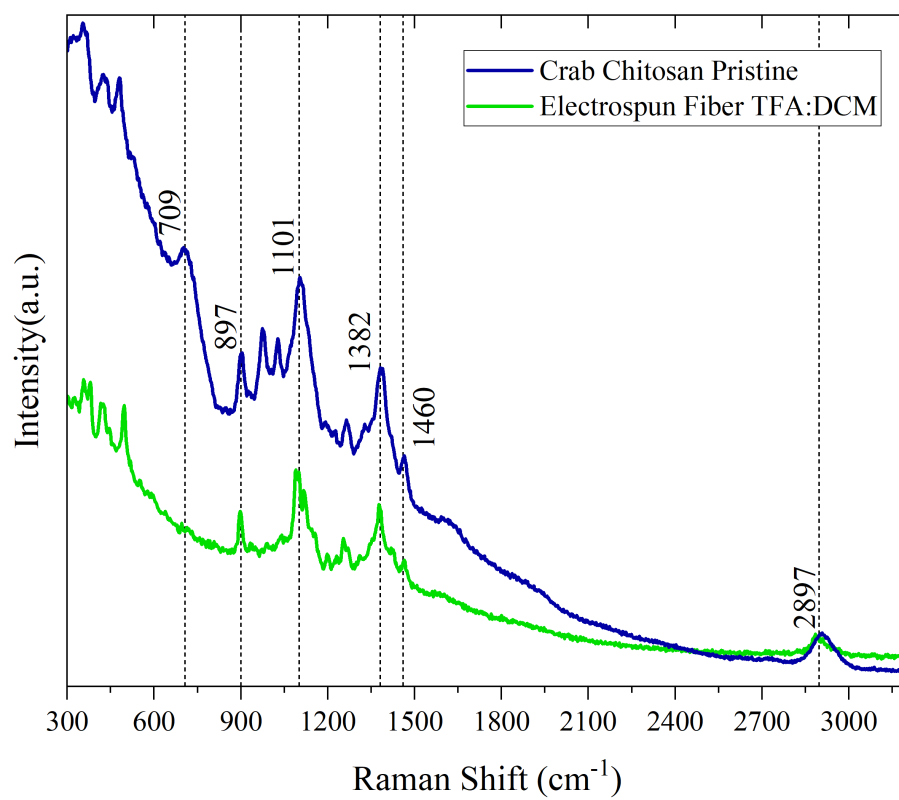


Figure 4.16: Raman spectra of crab chitosan fibers made by electrospinning TFA:DCM

Chapter 5

Conclusions & Outlook

The thesis research aims to develop a novel chitosan-based fibrous material using electrospinning techniques and explore its properties. This will help design chitosan-based materials with better stability for various biomedical applications. The research achieved its goal and discovered new information on designing chitosan-based materials.

In section 4.1 of Chapter 4, various parameters that are required for producing electrospun fibers were analyzed. The electrospinning process is quite complex, and multiple parameters must be examined. It is impossible to predict the fiber diameter or any other product characteristic based on a single parameter since many of these parameters are interrelated. To achieve the solution electrospinning, there were two control points. The first was ensuring the chitosan solution had the appropriate viscosity and conductivity for the electrospinning process. After several tests, it was determined that the AcOH solvent can dissolve the three types of chitosan used in this research. The polymer dissolution time is directly proportional to the molecular weight of the chitosan used.

The second control point is related to the electrospinning parameters. Despite attempts to use AcOH, electrospun fibers could not be obtained. The addition of the chitosan-MWCNT composite to increase

solution conductivity was unsuccessful. However, changing the solvent to TFA allowed for successful fiber production. This demonstrates that the polymer concentration factor in electrospinning is affected by the amount of polymer and the interaction between polymer and solvent. The switch to TFA was the key to success. During the electrospinning process, we experimented with different working parameters to determine the optimal combination that yields favorable outcomes: needle diameter (0.35mm-0.9mm), collector distance (6cm-15cm), flow rate (0.05 ml/h-0.1 ml/h) and voltage (6 kV-20 kV)

Chapter 4, Section 4.2 indicates that cosolvent produces smooth-looking fibers without droplets. The best-looking fibers were achieved by electrospinning a 4% w/v chitosan (Sigma Aldrich and crab) with TFA: DCM 70:30, using high voltage and low flow rate. Fibers made from Sigma-Aldrich chitosan had an average diameter of 1,4 μm and fibers made from crab chitosan had an average diameter of 2,34 μm . This study shows that TFA serves as both a solvent and proton donor, which helps to disperse chitosan and reduce repulsive forces during electrospinning. As a result, it promotes the formation of fibers. The appearance of the fibers was improved by using a TFA:DCM 70:30 cosolvent which by lowering the boiling point of the solution allows for successful electrospinning.

In Section 4.3, Raman spectroscopy showed that chitosan nanofibers with amide groups have a stable structure. Raman investigations prove that the electrospinning process can not change the chemical nature of the polymer. Raman spectra of the processed samples showed the characteristic functional groups of chitosan. The peaks were assigned as follows: Amide I (1659-2891 cm^{-1}), Amide III (1659 cm^{-1}), C-H (1200-1300 cm^{-1}), OH (426 cm^{-1}), CO-NH₂ (493 cm^{-1}), C-O-C (896 cm^{-1}) and O-H (1101 cm^{-1}). Also, the solvent-related peaks (CF₃) in the spectra were not distinctly visible, indicating that the electrospinning process had effectively evaporated all the solvent, thus yielding stable chitosan fibers

Electrospinning biological materials demands less flexibility than synthetic polymers due to the sensitivity of biological materials that require a solvent that won't cause any harm. Chitosan, in particular, is extremely vulnerable to failure, and that's why it's crucial to opt for a solvent that guarantees the stability

of the polymer during the electrospinning process.

In summary, this thesis research contributes significantly to the design of chitosan fibers with various physicochemical properties through electrospinning. The polymer could not be electrolylated using AcOH as solvent. This challenge was addressed by changing the solvent to TFA, which is anticipated to improve the conditions for electrospinning of natural polymers. Moreover, the structure of chitosan fibers was studied by conventional characterization methods and Raman spectral imaging. The findings presented here offer a thorough comprehension of how supramolecular assembly contributes to the creation of electrospun fibers using chitosan. These insights can inform the development of fresh material design tactics for chitosan electrospun fibers.

5.1 Recommendations and future work

In addition to fibers, trifluoroacetic acid (TFA) can also be used for producing chitosan thin films. This study demonstrated TFA's high volatility, which is advantageous for biomaterial production. Also, to ensure the complete dissolution of the polymer, it is advised to prepare the solutions a day prior to electrospinning. This approach eliminates the need for heating plates, which can lead to degradation of chitosan at high temperatures ($>45^{\circ}\text{C}$). It is also recommended to characterize the fibers as soon as possible to prevent any damage. The next step of this research is to improve the physical properties of the fibers to perform cell growth and proliferation assessment.

Appendix A

Electrospinning processing data

Solvent	Polymer	Solution Concentration % (w/v)	Needle diameter(mm)	Collection Distance (cm)	Flow rate (mL/Hr)	Voltage (kV)
AcOH	Commercial Chitosan	2	0,35	6	0,1	8-15
					0,5	8-15
				8	0,1	8-15
					0,5	11-15
				10	0,1	8-15
					0,5	11-15
			0,45	6	0,1	8-15
					0,5	8-15
				8	0,1	8-15
					0,5	11-15
				10	0,1	8-15
					0,5	11-15
		0,7	6	0,1	8-15	
				0,5	11-15	
			8	0,1	8-15	
				0,5	11-15	
			10	0,1	8-15	
				0,5	11-15	
		2,5	0,35	6	0,1	8-15
					0,5	8-15
				8	0,1	8-15
					0,5	11-15
				10	0,1	8-15
					0,5	8-15
			0,45	6	0,1	8-15
					0,5	8-15
				8	0,1	8-15
					0,5	8-15
				10	0,1	8-15
					0,5	11-15
		0,7	10	0,1	8-15	
				0,5	8-15	
			8	0,1	8-15	
				0,5	8-15	
			10	0,1	8-15	
				0,5	11-15	
		3	0,35	6	0,1	8-15
					0,5	8-15
				8	0,1	8-15
					0,5	8-15
				10	0,1	8-15
					0,5	8-15
			0,45	6	0,1	8-15
					0,5	8-15
				8	0,1	8-15
					0,5	8-15
				10	0,1	8-15
					0,5	8-15
0,7	10	0,1	8-15			
		0,5	8-15			
	8	0,1	8-15			
		0,5	8-15			
	10	0,1	8-15			
		0,5	8-15			

Table A.1: ACOH Commercial chitosan samples

Solvent	Polymer	Solution Concentration % (w/v)	Needle diameter(mm)	Collection Distance (cm)	Flow rate (mL/Hr)	Voltage (kV)
AcOH	Shrimp Chitosan	6	0,45	6	0,1	11-15
					0,5	11-15
				8	0,1	11-15
					0,5	11-15
				10	0,1	11-15
					0,5	11-15
			0,7	6	0,1	11-15
					0,5	11-15
				8	0,1	11-15
					0,5	11-15
				10	0,1	11-15
					0,5	11-15
		0,9	6	0,1	11-15	
				0,5	11-15	
			8	0,1	11-15	
				0,5	11-15	
			10	0,1	11-15	
				0,5	11-15	
		7	0,45	6	0,1	11-15
					0,5	11-15
				8	0,1	11-15
					0,5	11-15
				10	0,1	11-15
					0,5	11-15
			0,7	6	0,1	11-15
					0,5	11-15
				8	0,1	11-15
					0,5	11-15
				10	0,1	11-15
					0,5	11-15
		0,9	10	0,1	11-15	
				0,5	11-15	
			8	0,1	11-15	
				0,5	11-15	
			10	0,1	11-15	
				0,5	11-15	
		8	0,45	6	0,1	11-15
					0,5	11-15
				8	0,1	11-15
					0,5	11-15
				10	0,1	11-15
					0,5	11-15
			0,7	6	0,1	11-15
					0,5	11-15
				8	0,1	11-15
					0,5	11-15
				10	0,1	11-15
					0,5	11-15
0,9	10	0,1	11-15			
		0,5	11-15			
	8	0,1	11-15			
		0,5	11-15			
	10	0,1	11-15			
		0,5	11-15			

Table A.2: ACOH Shrimp Chitosan Samples

Solvent	Polymer	Solution Concentration % (w/v)	Needle diameter (mm)	Collection Distance (cm)	Flow rate (mL/Hr)	Voltage (kV)
AcOH	Crab Chitosan	3	0.45	6	0.1	11-15
					0.5	11-15
				8	0.1	11-15
					0.5	11-15
				10	0.1	11-15
					0.5	11-15
			0.7	6	0.1	11-15
					0.5	11-15
				8	0.1	11-15
					0.5	11-15
				10	0.1	11-15
					0.5	11-15
		0.9	6	0.1	11-15	
				0.5	11-15	
			8	0.1	11-15	
				0.5	11-15	
			10	0.1	11-15	
				0.5	11-15	
		4	0.45	6	0.1	11-15
					0.5	11-15
				8	0.1	11-15
					0.5	11-15
				10	0.1	11-15
					0.5	11-15
			0.7	6	0.1	11-15
					0.5	11-15
				8	0.1	11-15
					0.5	11-15
				10	0.1	11-15
					0.5	11-15
			0.9	10	0.1	11-15
					0.5	11-15
				8	0.1	11-15
					0.5	11-15
				10	0.1	11-15
					0.5	11-15
		5	0.45	6	0.1	11-15
					0.5	11-15
				8	0.1	11-15
					0.5	11-15
				10	0.1	11-15
					0.5	11-15
			0.7	6	0.1	11-15
					0.5	11-15
				8	0.1	11-15
					0.5	11-15
				10	0.1	11-15
					0.5	11-15
0.9	10		0.1	11-15		
			0.5	11-15		
	8		0.1	11-15		
			0.5	11-15		
	10		0.1	11-15		
			0.5	11-15		

Table A.3: ACOH Crab chitosan Samples

Solvent	Polymer	Solution Concentration% (w/v)	Needle diameter(mm)	Collection Distance(cm)	Flow rate(mL/Hr)	Voltage(kV)
AcOH	Commercial Chitosan+MWCNT	2	0,35	6	0,1	11-15
					0,5	11-15
				8	0,1	11-15
					0,5	11-15
				10	0,1	11-15
					0,5	11-15
			0,45	6	0,1	11-15
					0,5	11-15
				8	0,1	11-15
					0,5	11-15
				10	0,1	11-15
					0,5	11-15
		0,7	6	0,1	11-15	
				0,5	11-15	
			8	0,1	11-15	
				0,5	11-15	
			10	0,1	11-15	
				0,5	11-15	
		2,5	0,35	6	0,1	11-15
					0,5	11-15
				8	0,1	11-15
					0,5	11-15
				10	0,1	11-15
					0,5	11-15
			0,45	6	0,1	11-15
					0,5	11-15
				8	0,1	11-15
					0,5	11-15
				10	0,1	11-15
					0,5	11-15
		0,7	10	0,1	11-15	
				0,5	11-15	
			8	0,1	11-15	
				0,5	11-15	
			10	0,1	11-15	
				0,5	11-15	
		3	0,35	6	0,1	11-15
					0,5	11-15
				8	0,1	11-15
					0,5	11-15
				10	0,1	11-15
					0,5	11-15
			0,45	6	0,1	11-15
					0,5	11-15
				8	0,1	11-15
					0,5	11-15
				10	0,1	11-15
					0,5	11-15
0,7	10	0,1	11-15			
		0,5	11-15			
	8	0,1	11-15			
		0,5	11-15			
	10	0,1	11-15			
		0,5	11-15			

Table A.4: ACOH Commercial chitosan+MWCNT samples

Solvent	Polymer	Solution Concentration%(w/v)	Needle diameter(mm)	Collection Distance(cm)	Flow rate(mL/Hr)	Voltage(kV)
AcOH	Shrimp Chitosan+MWCNT	6	0,45	6	0,1	11-15
					0,5	11-15
				8	0,1	11-15
					0,5	11-15
				10	0,1	11-15
					0,5	11-15
			0,7	6	0,1	11-15
					0,5	11-15
				8	0,1	11-15
					0,5	11-15
				10	0,1	11-15
					0,5	11-15
		0,9	6	0,1	11-15	
				0,5	11-15	
			8	0,1	11-15	
				0,5	11-15	
			10	0,1	11-15	
				0,5	11-15	
		7	0,45	6	0,1	11-15
					0,5	11-15
				8	0,1	11-15
					0,5	11-15
				10	0,1	11-15
					0,5	11-15
			0,7	6	0,1	11-15
					0,5	11-15
				8	0,1	11-15
					0,5	11-15
				10	0,1	11-15
					0,5	11-15
		0,9	10	0,1	11-15	
				0,5	11-15	
			8	0,1	11-15	
				0,5	11-15	
			10	0,1	11-15	
				0,5	11-15	
		8	0,45	6	0,1	11-15
					0,5	11-15
				8	0,1	11-15
					0,5	11-15
				10	0,1	11-15
					0,5	11-15
			0,7	6	0,1	11-15
					0,5	11-15
				8	0,1	11-15
					0,5	11-15
				10	0,1	11-15
					0,5	11-15
0,9	10	0,1	11-15			
		0,5	11-15			
	8	0,1	11-15			
		0,5	11-15			
	10	0,1	11-15			
		0,5	11-15			

Table A.5: ACOH Shrimp chitosan+MWCNT samples

Solvent	Polymer	Solution Concentration % (w/v)	Needle diameter(mm)	Collection Distance(cm)	Flow rate(mL/Hr)	Voltage(kV)
AcOH	Crab Chitosan+MWCNT	3	0.45	6	0.1	11-15
					0.5	11-15
				8	0.1	11-15
					0.5	11-15
				10	0.1	11-15
					0.5	11-15
			0.7	6	0.1	11-15
					0.5	11-15
				8	0.1	11-15
					0.5	11-15
				10	0.1	11-15
					0.5	11-15
		0.9	6	0.1	11-15	
				0.5	11-15	
			8	0.1	11-15	
				0.5	11-15	
			10	0.1	11-15	
				0.5	11-15	
		4	0.45	6	0.1	11-15
					0.5	11-15
				8	0.1	11-15
					0.5	11-15
				10	0.1	11-15
					0.5	11-15
			0.7	6	0.1	11-15
					0.5	11-15
				8	0.1	11-15
					0.5	11-15
				10	0.1	11-15
					0.5	11-15
		0.9	10	0.1	11-15	
				0.5	11-15	
			8	0.1	11-15	
				0.5	11-15	
			10	0.1	11-15	
				0.5	11-15	
		5	0.45	6	0.1	11-15
					0.5	11-15
				8	0.1	11-15
					0.5	11-15
				10	0.1	11-15
					0.5	11-15
			0.7	6	0.1	11-15
					0.5	11-15
				8	0.1	11-15
					0.5	11-15
				10	0.1	11-15
					0.5	11-15
0.9	10	0.1	11-15			
		0.5	11-15			
	8	0.1	11-15			
		0.5	11-15			
	10	0.1	11-15			
		0.5	11-15			

Table A.6: ACOH Crab chitosan+MWCNT samples

Solvent	Polymer	Solution Concentration % (w/v)	Needle diameter(mm)	Collection Distance(cm)	Flow rate(mL/Hr)	Voltage(kV)
TFA	Commercial Chitosan	2	0,35	6	0,1	11-15
					0,5	11-15
				8	0,1	11-15
					0,5	12-15
				10	0,1	11-15
					0,5	12-15
			0,45	6	0,1	12-15
					0,5	11-15
				8	0,1	11-15
					0,5	14-15
				10	0,1	11-15
					0,5	11-15
		0,7	6	0,1	14-15	
				0,5	11-15	
			8	0,1	14-15	
				0,5	11-15	
			10	0,1	14-15	
				0,5	11-15	
		2,5	0,35	6	0,1	11-15
					0,5	11-15
				8	0,1	11-15
					0,5	11-15
				10	0,1	11-15
					0,5	11-15
			0,45	6	0,1	11-15
					0,5	11-15
				8	0,1	11-15
					0,5	11-15
				10	0,1	11-15
					0,5	11-15
		0,7	10	0,1	11-15	
				0,5	11-15	
			8	0,1	11-15	
				0,5	11-15	
			10	0,1	11-15	
				0,5	11-15	
		3	0,35	6	0,1	11-15
					0,5	11-15
				8	0,1	11-15
					0,5	11-15
				10	0,1	11-15
					0,5	11-15
			0,45	6	0,1	11-15
					0,5	11-15
				8	0,1	11-15
					0,5	11-15
				10	0,1	11-15
					0,5	11-15
0,7	10	0,1	11-15			
		0,5	11-15			
	8	0,1	11-15			
		0,5	11-15			
	10	0,1	11-15			
		0,5	11-15			

Table A.7: TFA Commercial chitosan samples

Solvent	Polymer	Solution Concentration % (w/v)	Needle diameter(mm)	Collection Distance(cm)	Flow rate(mL/Hr)	Voltage(kV)
TFA	Crab Chitosan	3	0,45	6	0,1	11-15
					0,5	11-15
				8	0,1	11-15
					0,5	11-15
				10	0,1	11-15
					0,5	11-15
			0,7	6	0,1	11-15
					0,5	11-15
				8	0,1	11-15
					0,5	11-15
				10	0,1	11-15
					0,5	11-15
		0,9	6	0,1	11-15	
				0,5	11-15	
			8	0,1	11-15	
				0,5	11-15	
			10	0,1	11-15	
				0,5	11-15	
		4	0,45	6	0,1	11-15
					0,5	11-15
				8	0,1	11-15
					0,5	11-15
				10	0,1	11-15
					0,5	11-15
			0,7	6	0,1	11-15
					0,5	11-15
				8	0,1	11-15
					0,5	11-15
				10	0,1	11-15
					0,5	11-15
		0,9	10	0,1	11-15	
				0,5	11-15	
			8	0,1	11-15	
				0,5	11-15	
			10	0,1	11-15	
				0,5	11-15	
		5	0,45	6	0,1	11-15
					0,5	11-15
				8	0,1	11-15
					0,5	11-15
				10	0,1	11-15
					0,5	11-15
			0,7	6	0,1	11-15
					0,5	11-15
				8	0,1	11-15
					0,5	11-15
				10	0,1	11-15
					0,5	11-15
0,9	10	0,1	11-15			
		0,5	11-15			
	8	0,1	11-15			
		0,5	11-15			
	10	0,1	11-15			
		0,5	11-15			

Table A.8: TFA Crab chitosan samples

Solvent	Polymer	Solution Concentration % (w/v)	Needle diameter(mm)	Collection Distance(cm)	Flow rate(mL/Hr)	Voltage(kV)
TFA/DCM	Commercial Chitosan	2	0,35	6	0,1	11-15
					0,5	11-15
				8	0,1	11-15
					0,5	11-15
				10	0,1	11-15
					0,5	11-15
			0,45	6	0,1	11-15
					0,5	11-15
				8	0,1	11-15
					0,5	11-15
				10	0,1	11-15
					0,5	11-15
		0,7	6	0,1	11-15	
				0,5	11-15	
			8	0,1	11-15	
				0,5	11-15	
			10	0,1	11-15	
				0,5	11-15	
		2,5	0,35	6	0,1	11-15
					0,5	11-15
				8	0,1	11-15
					0,5	11-15
				10	0,1	11-15
					0,5	11-15
			0,45	6	0,1	11-15
					0,5	11-15
				8	0,1	11-15
					0,5	11-15
				10	0,1	11-15
					0,5	11-15
		0,7	10	0,1	11-15	
				0,5	11-15	
			8	0,1	11-15	
				0,5	11-15	
			10	0,1	11-15	
				0,5	11-15	
		3	0,35	6	0,1	11-15
					0,5	11-15
				8	0,1	11-15
					0,5	11-15
				10	0,1	11-15
					0,5	11-15
			0,45	6	0,1	11-15
					0,5	11-15
				8	0,1	11-15
					0,5	11-15
				10	0,1	11-15
					0,5	11-15
0,7	10	0,1	11-15			
		0,5	11-15			
	8	0,1	11-15			
		0,5	11-15			
	10	0,1	11-15			
		0,5	11-15			

Table A.9: TFA/DCM Commercial chitosan samples

Solvent	Polymer	Solution Concentration%(w/v)	Needle diameter(mm)	Collection Distance(cm)	Flow rate (mL/Hr)	Voltage(kV)
TFA/DCM	Crab Chitosan	3	0,45	6	0,1	11-15
					0,5	11-15
				8	0,1	11-15
					0,5	11-15
			10	0,1	11-15	
				0,5	11-15	
			0,7	6	0,1	11-15
					0,5	11-15
				8	0,1	11-15
					0,5	11-15
				10	0,1	11-15
					0,5	11-15
		0,9	6	0,1	11-15	
				0,5	11-15	
			8	0,1	11-15	
				0,5	11-15	
			10	0,1	11-15	
				0,5	11-15	
		4	0,45	6	0,1	11-15
					0,5	11-15
				8	0,1	11-15
					0,5	11-15
				10	0,1	11-15
					0,5	11-15
			0,7	6	0,1	11-15
					0,5	11-15
				8	0,1	11-15
					0,5	11-15
				10	0,1	11-15
					0,5	11-15
		0,9	10	0,1	15-17	
				0,5	15-17	
			8	0,1	15-17	
				0,5	11-15	
			10	0,1	15-17	
				0,5	11-15	
		5	0,45	6	0,1	15-17
					0,5	15-17
				8	0,1	15-17
					0,5	15-17
				10	0,1	15-17
					0,5	15-17
			0,7	6	0,1	15-17
					0,5	15-17
				8	0,1	15-17
					0,5	15-17
				10	0,1	15-17
					0,5	15-17
0,9	10	0,1	15-17			
		0,5	15-17			
	8	0,1	15-17			
		0,5	15-17			
	10	0,1	15-17			
		0,5	15-17			

Table A.10: TFA/DCM Crab chitosan samples

Appendix B

WET SPINNING

Since it was not possible to obtain fibers by the electrospinning method using AcOH as a solvent, it was decided to produce fibers by the wet spinning method following the methodology proposed by Nechyporchuk²⁷ and evaluate the morphology and chemical structure of the resulting fibers. Chitosan solutions were injected into a coagulation bath to form fibers. The wet spinning experiments were performed with chitosan solution having the concentration 2.5 % (w/w) and sodium hydroxide solutions with concentration 1.5 (mol/L). The chitosan solutions were transferred to a 1 mL syringe and injected into the coagulation bath to form the chitosan fibers. The residence time for coagulation was 5 min. The neutralization reaction between the $-NH_3^+$ groups and NaOH is instantaneous. Table B.1 shows the images of the fibers obtained by the wet spinning process. Defined fibers with an average diameter of 300 μm are observed.

Figure B.1 shows the Raman spectrum of the fiber that was formed by the wet spinning process and the spectrum of Sigma Aldrich's pristine chitosan. The chitosan fiber's spectrum differs from the pristine material, as seen in the Raman results. The fiber loses characteristic peaks of the chitosan molecule, therefore, some bands are not active in fiber but are active in pristine Raman band

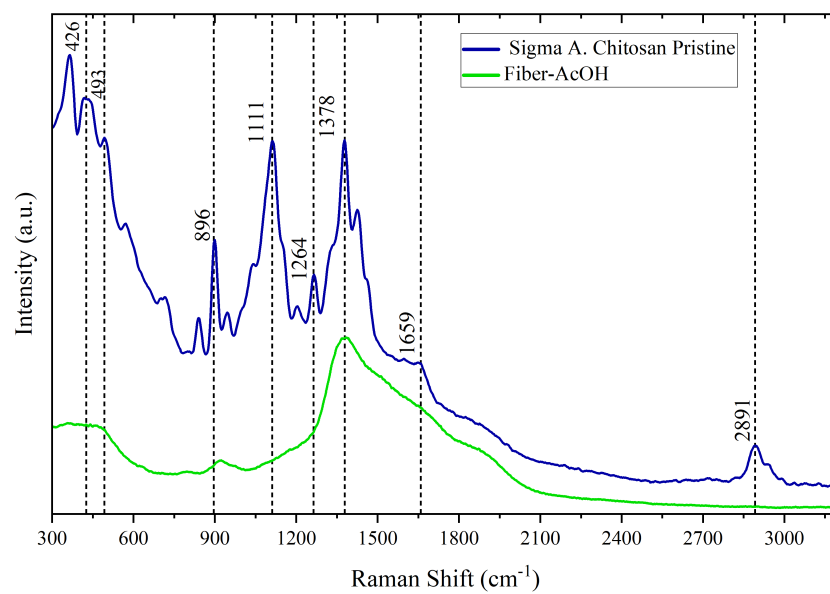


Figure B.1: Raman Spectra of Sigma Aldrich chitosan fibers made by wet spinning

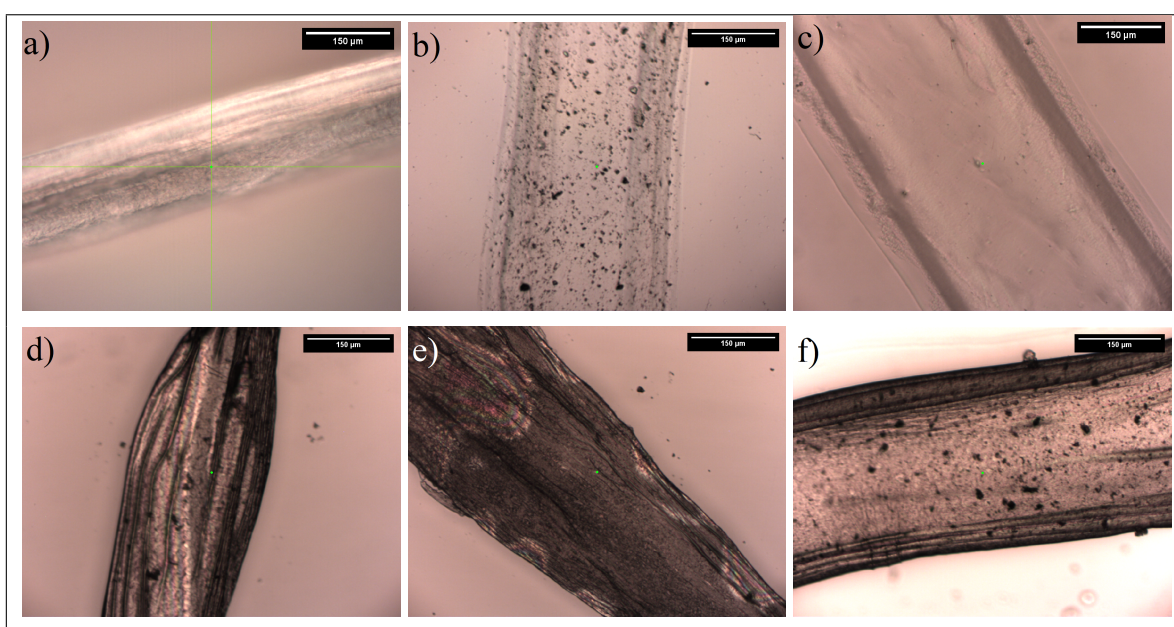


Table B.1: Chitosan fiber made by the wet spinning technique using AcOh as solvent. (a)Sigma-Aldrich, (b)Sigma-Aldrich+MWCNT, (c)Shrimp, (d)Shrimp+MWCNT, (e) Crab and, (f)Crab+MWCNT

Bibliography

- [1] Sun, K.; Li, Z. H. Preparations, properties and applications of chitosan based nanofibers fabricated by electrospinning. *Express Polymer Letters* **2011**, *5*, 342–361.
- [2] Elsabee, M. Z.; Naguib, H. F.; Morsi, R. E. Chitosan based nanofibers, review. *Materials Science and Engineering C* **2012**, *32*, 1711–1726.
- [3] Sakkara, S.; Santosh, S.; Reddy, N. Chitosan Fibers. **2020**,
- [4] Li, X. Q.; Tang, R. C. Crosslinking of chitosan fiber by a water-soluble diepoxy crosslinker for enhanced acid resistance and its impact on fiber structures and properties. *Reactive and Functional Polymers* **2016**, *100*, 116–122.
- [5] Yang, S.; Zhang, X.; Zhang, D. Electrospun chitosan/poly (vinyl alcohol)/graphene oxide nanofibrous membrane with ciprofloxacin antibiotic drug for potential wound dressing application. *International Journal of Molecular Sciences* **2019**, *20*.
- [6] Croisier, F.; Jérôme, C. Chitosan-based biomaterials for tissue engineering. *European Polymer Journal* **2013**, *49*, 780–792.
- [7] Pal, P.; Pal, A.; Nakashima, K.; Yadav, B. K. Applications of chitosan in environmental remediation: A review. *Chemosphere* **2021**, *266*.

- [8] Sangsanoh, P.; Supaphol, P. Stability improvement of electrospun chitosan nanofibrous membranes in neutral or weak basic aqueous solutions. *Biomacromolecules* **2006**, *7*, 2710–2714.
- [9] Schiffman, J. D.; Schauer, C. L. Cross-linking chitosan nanofibers. *Biomacromolecules* **2007**, *8*, 594–601.
- [10] Camara Nacional de Acuicultura. 2020; <https://www.cna-ecuador.com/>.
- [11] D, R.; A, S.; S, S. Potential Recovery of Protein from Shrimp Waste in Aqueous two Phase System. 2012; www.isca.in.
- [12] Gieroba, B.; Sroka-Bartnicka, A.; Kazimierzak, P.; Kalisz, G.; Lewalska-Graczyk, A.; Vivcharenko, V.; Nowakowski, R.; Pieta, I. S.; Przekora, A. Surface Chemical and Morphological Analysis of Chitosan/1,3--D-Glucan Polysaccharide Films Cross-linked at 90 °C. *International Journal of Molecular Sciences* **2022**, *23*.
- [13] Dhayal, V.; Hashmi, S. Z.; Kumar, U.; Choudhary, B. L.; Kuznetsov, A. E.; Dalela, S.; Kumar, S.; Kaya, S.; Dolia, S. N.; Alvi, P. A. Spectroscopic studies, molecular structure optimization and investigation of structural and electrical properties of novel and biodegradable Chitosan-GO polymer nanocomposites. *Journal of Materials Science* **2020**, *55*, 14829–14847.
- [14] Ashraf, H.; Asran, S.; Sayed, A. Martin-Luther-Universität Halle-Wittenberg Electrospinning of polymeric nanofibers and nanocomposite materials: Fabrication, physicochemical characterization and medical applications. 2011.
- [15] Mohammadkhani, G.; Ramamoorthy, S. K.; Adolfsson, K. H.; Mahboubi, A.; Hakkarainen, M.; Zamani, A. New solvent and coagulating agent for development of Chitosan fibers by wet spinning. *Polymers* **2021**, *13*.
- [16] Sinha, N.; Ma, J.; Yeow, J. T. W. Carbon Nanotube-Based Sensors. *J. Nanosci. Nanotechnol.* **2006**, *6*, 573.

- [17] Raafat, D.; Bargaen, K. V.; Haas, A.; Sahl, H. G. Insights into the mode of action of chitosan as an antibacterial compound. *Applied and Environmental Microbiology* **2008**, *74*, 3764–3773.
- [18] East, G. C.; Qint, Y. Wet Spinning of Chitosan and the Acetylation of Chitosan Fibers.
- [19] Burns, N. A.; Burroughs, M. C.; Gracz, H.; Pritchard, C. Q.; Brozena, A. H.; Willoughby, J.; Khan, S. A. Cyclodextrin facilitated electrospun chitosan nanofibers. *RSC Advances* **2015**, *5*, 7131–7137.
- [20] Nirmala, R.; Il, B. W.; Navamathavan, R.; El-Newehy, M. H.; Kim, H. Y. Preparation and characterizations of anisotropic chitosan nanofibers via electrospinning. *Macromolecular Research* **2011**, *19*, 345–350.
- [21] Ren, X. D.; Liu, Q. S.; Feng, H.; Yin, X. Y. The characterization of chitosan nanoparticles by raman spectroscopy. *Applied Mechanics and Materials* **2014**, *665*, 367–370.
- [22] Torres-Giner, S.; Ocio, M. J.; Lagaron, J. M. Development of active antimicrobial fiber based chitosan polysaccharide nanostructures using electrospinning. *Engineering in Life Sciences* **2008**, *8*, 303–314.
- [23] de Andrade, S. M. B.; Ladchumananandasivam, R.; da Rocha, B. G.; Belarmino, D. D.; Galvão, A. O. The Use of Exoskeletons of Shrimp (*Litopenaeus vanammei*) and Crab (*Ucides cordatus*) for the Extraction of Chitosan and Production of Nanomembrane. *Materials Sciences and Applications* **2012**, *03*, 495–508.
- [24] Xue, C.; Wilson, L. D. A spectroscopic study of solid-phase chitosan/cyclodextrin-based electrospun fibers. *Fibers* **2019**, *7*.
- [25] Korniienko, V.; Husak, Y.; Yanovska, A.; Banasiuk, R.; Yusupova, A.; Savchenko, A.; Holubnycha, V.; Pogorielov, M. Functional and biological characterization of chitosan electrospun nanofibrous membrane nucleated with silver nanoparticles. *Applied Nanoscience (Switzerland)* **2022**, *12*, 1061–1070.

- [26] Kim, C. H.; Park, H.-S.; Gin, Y. J.; Son, Y.; Lim, S.-H.; Choi, Y. J.; Park, K.-S.; Park, C. W. Improvement of the Biocompatibility of Chitosan Dermal Scaffold by Rigorous Dry Heat Treatment. *Macromolecular Research* **2004**, *12*, 367–373.
- [27] Nechyporchuk, O.; Nilsson, T. Y.; Ulmefors, H.; Köhnke, T. Wet Spinning of Chitosan Fibers: Effect of Sodium Dodecyl Sulfate Adsorption and Enhanced Dope Temperature. *ACS Applied Polymer Materials* **2020**, *2*, 3867–3875.
- [28] Morin-Crini, N.; Lichtfouse, E.; Torri, G.; Crini, G. Applications of chitosan in food, pharmaceuticals, medicine, cosmetics, agriculture, textiles, pulp and paper, biotechnology, and environmental chemistry. 2019.
- [29] Baranwal, A.; Kumar, A.; Priyadarshini, A.; Oggu, G. S.; Bhatnagar, I.; Srivastava, A.; Chandra, P. Chitosan: An undisputed bio-fabrication material for tissue engineering and bio-sensing applications. *International Journal of Biological Macromolecules* **2018**, *110*, 110–123.
- [30] Negm, N. A.; Hefni, H. H.; Abd-Elaal, A. A.; Badr, E. A.; Kana, M. T. A. Advancement on modification of chitosan biopolymer and its potential applications. 2020.
- [31] Antaby, E.; Klinkhammer, K.; Sabantina, L. Electrospinning of chitosan for antibacterial applications—current trends. *Applied Sciences (Switzerland)* **2021**, *11*.
- [32] Mourya, V. K.; Inamdar, N. N. Chitosan-modifications and applications: Opportunities galore. 2008.
- [33] Kumar, M. N. V. R. A review of chitin and chitosan applications. *Reactive Functional Polymers* **2000**, *46*, 1–27.
- [34] Bhardwaj, N.; Kundu, S. C. Electrospinning: A fascinating fiber fabrication technique. 2010.
- [35] Haghi, A. K.; Akbari, M. Trends in electrospinning of natural nanofibers. 2007.
- [36] Rezaei, F. S.; Sharifianjazi, F.; Esmailkhanian, A.; Salehi, E. Chitosan films and scaffolds for regenerative medicine applications: A review. 2021.

- [37] Fatullayeva, S.; Tagiyev, D.; Zeynalov, N.; Mammadova, S.; Aliyeva, E. Recent advances of chitosan-based polymers in biomedical applications and environmental protection. 2022.
- [38] Ömer Bahadır Mergen,; Arda, E.; Evingür, G. A. Electrical, optical and mechanical properties of chitosan biocomposites. *Journal of Composite Materials* **2020**, *54*, 1497–1510.
- [39] Ohkawa, K.; Cha, D.; Kim, H.; Nishida, A.; Yamamoto, H. Electrospinning of chitosan. *Macromolecular Rapid Communications* **2004**, *25*, 1600–1605.
- [40] Estevinho, B. N.; Rocha, F.; Santos, L.; Alves, A. Microencapsulation with chitosan by spray drying for industry applications - A review. 2013.
- [41] Gu, B. K.; Park, S. J.; Kim, M. S.; Kang, C. M.; Kim, J. I.; Kim, C. H. Fabrication of sonicated chitosan nanofiber mat with enlarged porosity for use as hemostatic materials. *Carbohydrate Polymers* **2013**, *97*, 65–73.
- [42] Ribeiro, A. S.; Costa, S. M.; Ferreira, D. P.; Calhelha, R. C.; Barros, L.; Stojković, D.; Soković, M.; Ferreira, I. C.; Fangueiro, R. Chitosan/nanocellulose electrospun fibers with enhanced antibacterial and antifungal activity for wound dressing applications. *Reactive and Functional Polymers* **2021**, *159*.
- [43] Jo, G.-H.; Park, R.-D.; Jung, W.-J. *Enzymatic Production of Chitin from Crustacean Shell Waste*; CRC Press, 2010; pp 37–45.
- [44] Mistry, P. H.; Mohapatra, S. K.; Dash, A. K. Effect of high-pressure homogenization and stabilizers on the physicochemical properties of curcumin-loaded glycerol monooleate/chitosan nanostructures. *Nanomedicine* **2012**, *7*, 1863–1876.
- [45] Cui, C.; Sun, S.; Wu, S.; Chen, S.; Ma, J.; Zhou, F. Electrospun chitosan nanofibers for wound healing application. *Engineered Regeneration* **2021**, *2*, 82–90.

- [46] Moutsatsou, P.; Coopman, K.; Georgiadou, S. Chitosan Conductive PANI/Chitosan Composite Nanofibers - Evaluation of Antibacterial Properties. *Current Nanomaterials* **2018**, *4*, 6–20.
- [47] Escamilla-García, M.; Calderón-Domínguez, G.; Chanona-Pérez, J. J.; Farrera-Rebollo, R. R.; Andraca-Adame, J. A.; Arzate-Vázquez, I.; Mendez-Mendez, J. V.; Moreno-Ruiz, L. A. Physical and structural characterisation of zein and chitosan edible films using nanotechnology tools. *International Journal of Biological Macromolecules* **2013**, *61*, 196–203.
- [48] Rinaudo, M. Chitin and chitosan: Properties and applications. 2006.
- [49] Prashanth, K. V. H.; Tharanathan, R. N. Chitin/chitosan: modifications and their unlimited application potential-an overview. 2007.
- [50] Faldu, N. Scholarship at UWindsor Scholarship at UWindsor Electronic Theses and Dissertations Theses, Dissertations, and Major Papers Electrospinning of PEO Nanofibers Electrospinning of PEO Nanofibers. 2020; <https://scholar.uwindsor.ca/etd>.
- [51] Liao, X. Preparation and Properties of Electrospun Polyacrylonitrile Fiber Assemblies DISSERTATION.
- [52] Escamilla-García, M.; Calderón-Domínguez, G.; Chanona-Pérez, J. J.; Farrera-Rebollo, R. R.; Andraca-Adame, J. A.; Arzate-Vázquez, I.; Mendez-Mendez, J. V.; Moreno-Ruiz, L. A. Physical and structural characterisation of zein and chitosan edible films using nanotechnology tools. *International Journal of Biological Macromolecules* **2013**, *61*, 196–203.
- [53] Zajac, A.; Hanuza, J.; Wandas, M.; Dymińska, L. Determination of N-acetylation degree in chitosan using Raman spectroscopy. *Spectrochimica Acta - Part A: Molecular and Biomolecular Spectroscopy* **2015**, *134*, 114–120.
- [54] Al-Gharabli, S.; Al-Omari, B.; Kujawski, W.; Kujawa, J. Biomimetic hybrid membranes with covalently anchored chitosan – Material design, transport and separation. *Desalination* **2020**, *491*.

-
- [55] Al-Gharabli, S.; Al-Omari, B.; Kujawski, W.; Kujawa, J. Biomimetic hybrid membranes with covalently anchored chitosan – Material design, transport and separation. *Desalination* **2020**, *491*.
- [56] Aytaç, Z. ELECTROSPINNING of BIOCOMPATIBLE POLYMERIC NANOFIBERS FUNCTIONALIZED with CYCLODEXTRIN INCLUSION COMPLEX. 2012.